



Osteology of a New Specimen of *Macrocnemus* aff. *M. fuyuanensis* (Archosauromorpha, Protorosauria) from the Middle Triassic of Europe: Potential Implications for Species Recognition and Paleogeography of Tanystropheid Protorosaurs

OPEN ACCESS

Edited by:

Martin Daniel Ezcurra,
Bernardino Rivadavia Natural
Sciences Museum, Argentina

Reviewed by:

Richard J. Butler,
University of Birmingham,
United Kingdom
Adam Pritchard,
Smithsonian Institution (SI),
United States
Federico Agnolin,
Museo Argentino de Ciencias
Naturales, Argentina

*Correspondence:

Torsten M. Scheyer
tscheyer@pim.uzh.ch
orcid.org/0000-0002-6301-8983

Specialty section:

This article was submitted to
Paleontology,
a section of the journal
Frontiers in Earth Science

Received: 24 August 2017

Accepted: 30 October 2017

Published: 23 November 2017

Citation:

Jaquier VP, Fraser NC, Furrer H and
Scheyer TM (2017) Osteology of a
New Specimen of *Macrocnemus* aff.
M. fuyuanensis (Archosauromorpha,
Protorosauria) from the Middle Triassic
of Europe: Potential Implications for
Species Recognition and
Paleogeography of Tanystropheid
Protorosaurs. *Front. Earth Sci.* 5:91.
doi: 10.3389/feart.2017.00091

Vivien P. Jaquier¹, Nicholas C. Fraser², Heinz Furrer¹ and Torsten M. Scheyer^{1*}

¹ Paleontological Institute and Museum, University of Zurich, Zurich, Switzerland, ² National Museums Scotland, Edinburgh, United Kingdom

Over the past two decades, a wealth of marine and terrestrial reptiles, including protorosaurian archosauromorphs, has been described from Triassic shales and limestone layers in southern China. Recovered from the eastern margin of the Tethys Ocean, these forms often show remarkable similarities to taxa that were previously known and described from Europe, i.e., the western Tethyan margin. One protorosaurian that is known from the western and the eastern Tethyan province is the genus *Macrocnemus*, with currently three recognized species: (1) *Macrocnemus bassanii* from the Middle Triassic Besano Formation and Meride Limestone (late Anisian–early Ladinian), UNESCO World Heritage Site Monte San Giorgio, Ticino, Switzerland; (2) *Macrocnemus obristi* from the Prosanto Formation (early Ladinian) of the Ducan area, Grisons, Switzerland; and (3) *Macrocnemus fuyuanensis* from the Falang Formation (Ladinian), Yunnan Province, southern China. Recently a new specimen, PIMUZ T 1559, from the upper Besano Formation at Meride, Ticino, Switzerland, was prepared, revealing a disarticulated skeleton which includes most of the cranium and lower jaw, pre-caudal vertebral column and ribs, the forelimbs, and girdle elements. Unambiguously assignable to the genus *Macrocnemus*, it evinces particularly gracile elongated cervical ribs, as well as a humerus/radius ratio that is comparable only to that of *M. fuyuanensis* from southern China. Based on this feature we tentatively recognize the new specimen as *M. aff. fuyuanensis* from Europe. The position and exquisite preservation of the clavicle and interclavicle in this specimen allows a revision of the shoulder girdle of *Macrocnemus* when articulated, which also has implications for closely related protorosaurian taxa,

such as the long-necked *Tanystropheus*. Furthermore, differences in the shape and morphology of the interclavicle including pointed wing-like lateral processes and a short, fusiform caudal process represent rare discrete characters that allow separation of the specimens of *M. bassanii* from the new specimen of *M. aff. fuyuanensis*.

Keywords: anatomy, Tethys, Mesozoic, China, interclavicle, reptile, Tanystropheidae

INTRODUCTION

Protorosaurs are a group of archosauromorph reptiles characterized by their elongated cervical vertebrae and concomitantly elongated cervical ribs that frequently extend posteriorly across more than one intervertebral joint so that they form bundles of rib shafts. Among protorosaurs, *Macrocnemus* (Nopcsa, 1930), is a small lizard-like form restricted to the Middle Triassic (Anisian-Ladinian), but possibly extending into the Late Triassic (earliest Carnian; Jiang et al., 2011, p. 1230). The first species of *Macrocnemus* to be described was *Macrocnemus bassanii* (Nopcsa, 1930) from the Besano Formation at the Anisian-Ladinian boundary and the Cassina beds of the Meride Limestone (early Ladinian) of Monte San Giorgio, Canton Ticino, southern Switzerland and Province Varese, northern Italy (Nopcsa, 1931; Peyer, 1937; Rieppel, 1989). After an extensive description based on several fossil finds was published (Peyer, 1937), further details concerning the anatomy of *M. bassanii* were subsequently added (Kuhn-Schwyder, 1962; Rieppel and Gronowski, 1981; Rieppel, 1989; Premru, 1991; Renesto and Avanzini, 2002). In these previous studies, all specimens from the Swiss-Italian UNESCO World Heritage Site Monte San Giorgio were attributed to the species *M. bassanii*.

More recently two new species of *Macrocnemus* have been recognized in China and Switzerland, respectively. *Macrocnemus fuyuanensis* was described based on fossil finds from the Ladinian of the Zhuganpo Member of the Falang Formation, Fuyuan County of Yunnan Province in southern China (Li et al., 2007; Jiang et al., 2011). It differs from *M. bassanii* in having a considerably longer (~20%) humerus relative to the radius. Additional diagnostic characters were mentioned in the initial description of the species (“tibia shorter than femur” and “17 or 18 dorsal vertebrae”: Li et al., 2007, p. 1602; in addition a more slender pes compared to the hand was noted based on measurements of metacarpals/-tarsals IV). A re-examination of the holotype specimen IVPP V15001 and a new, referred specimen GMPKU-P-3001, however, concluded that the humerus/radius (H/R) ratio was the only unequivocal feature characteristic of *M. fuyuanensis* (Jiang et al., 2011). The third species, *Macrocnemus obristi*, was described based on two fragmentary posterior postcranial remains from the lower Ladinian of the Prosanto Formation in the Canton Graubünden in south-eastern Switzerland (Fraser and Furrer, 2013). This species has slender limbs and differs from the other two species by a considerably longer (i.e., 26%) tibia relative to the femur (tibia to femur ratio = T/F ratio).

Given the position of *Macrocnemus* as sister taxon to all remaining members of Tanystropheidae (sensu Pritchard et al., 2015; Ezcurra, 2016), understanding its detailed morphology

is important for character polarization at the base of this early archosauromorph clade. Furthermore, the temporal and spatial occurrences of the different specimens of *Macrocnemus* provide clues for understanding the biogeography in early Archosauromorpha. Here, we provide the first anatomical description of a well-preserved, but mostly disarticulated skeleton of *Macrocnemus* from the upper Besano Formation (PIMUZ T 1559), and compare it with existing species, to determine its taxonomic status. In addition, the Tethys-wide paleogeography of the different species of *Macrocnemus* is discussed and a revised, amended diagnosis for *Macrocnemus* and for the currently recognized species is summarized herein.

MATERIALS AND METHODS

PIMUZ T 1559 was found and excavated in 1956 during a systematic excavation directed by E. Kuhn-Schwyder (University of Zurich), in the upper Besano Formation (upper “Grenzbitumenzone,” *Secedensis* zone, late Anisian), at locality Mirigioli/point 902, near Meride, Monte San Giorgio, Canton Ticino, Switzerland. The reptile was discovered in a slab labeled only as “*Saurichthys* specimen,” but was only prepared between 2012 and 2014, at which time it was also X-rayed. The specimen consists of an associated skeleton (Figures 1A,B, Supplementary Figure 1), comprising a mostly disarticulated cranium, largely articulated but separate lower mandibles, an articulated portion of the cervical column consisting of four adjacent vertebrae, as well as other associated but disarticulated axial and appendicular elements. The specimen is preserved inside a laminated dolomite bed and was underlain by a disarticulated *Saurichthys* specimen (PIMUZ T 5753), which was partially prepared off the slab to reveal the scattered *Macrocnemus* bones. The respective positions of the scattered cranial, axial and appendicular elements on the slab indicate that the animal was embedded with the head and neck strongly bent backwards over the trunk region and therefore in a similar posture to PIMUZ T 2472, T 4822, and T 4355.

Direct comparison with another, yet only partially described, specimen previously referred to *M. bassanii*, PIMUZ T 2472 (Figure 1C), is undertaken herein. PIMUZ T 2472 was originally found by an excavation team led by B. Peyer in 1938, in the middle Besano Formation (middle “Grenzbitumenzone,” *Secedensis* zone, late Anisian) at the “oil shale” mine Tre Fontane near Meride, Monte San Giorgio, Canton Ticino, Switzerland. The specimen was first X-rayed and then subsequently prepared shortly prior to 1962, but only the skull was described (Kuhn-Schwyder, 1962), together with a comment that the postcranium of *M. bassanii* was already completely elucidated in Peyer’s previously published monographic work (Peyer, 1937). The

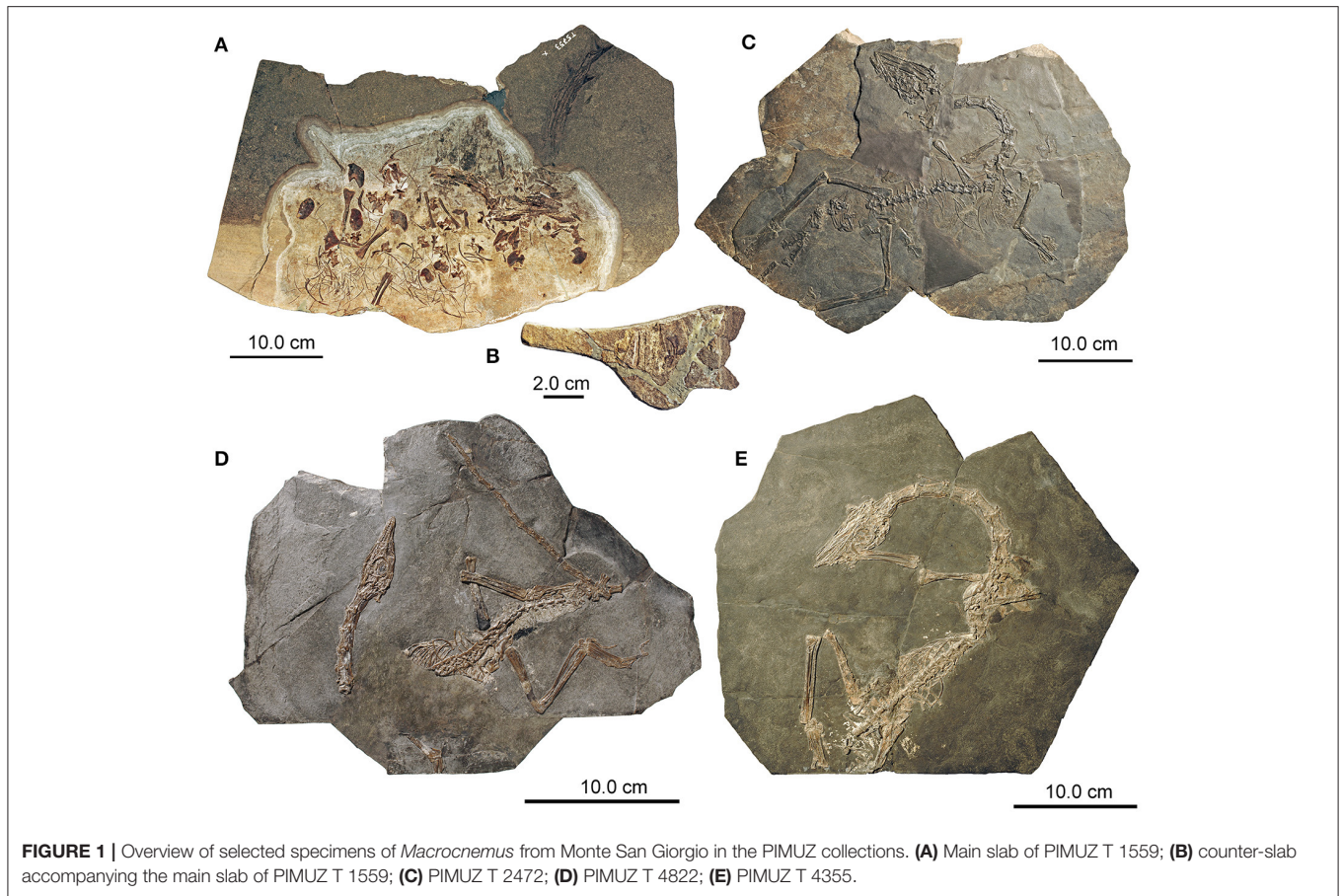


FIGURE 1 | Overview of selected specimens of *Macrocnemus* from Monte San Giorgio in the PIMUZ collections. **(A)** Main slab of PIMUZ T 1559; **(B)** counter-slab accompanying the main slab of PIMUZ T 1559; **(C)** PIMUZ T 2472; **(D)** PIMUZ T 4822; **(E)** PIMUZ T 4355.

specimen comprises the skull slightly separated from the vertebral column, the latter being largely in articulation until the sacral region; the distal part of the tail is not preserved. As noted by Kuhn-Schnyder (1962), the articulated left part of the skull is exposed in medial view and the skull roof in ventral view. The specimen furthermore has a disarticulated left forelimb but mostly articulated right forelimb, a mostly complete and articulated right hind limb and articulated stylopodial and zeugopodial elements of the left hind limb. The pectoral and pelvic girdle elements are all present but disarticulated. The anterior part of the skeleton (up to dorsal vertebra 10) is visible in right lateral view, whereas the posterior part has separated and rotated to be embedded mostly in ventral view. Other material used for comparison in this study included the more complete and overall articulated specimens PIMUZ T 4355 (**Figure 1D**) from the same locality Tre Fontane and PIMUZ T 4822 (**Figure 1E**) from the lower Ladinian Meride Limestone (Cassina beds), as well as data from the literature (e.g., Peyer, 1937; Premru, 1991; Li et al., 2007; Jiang et al., 2011). Comparison with the holotype PIMUZ A/III 1467 of *M. obristi* was limited, because of little overlap of the skeletal remains (Fraser and Furrer, 2013).

The *Macrocnemus* specimens were analyzed using a WILD Heerbrugg M8 microscope and measurements were taken using a PAV electronic caliper gauge 6511. Photographs were taken

with a NIKON D3X camera and Nikon AF-S Nikkor 24–70 mm lens. Images were processed with Adobe Creative Suite CS6. Measurements of PIMUZ T 1559 are compiled in a set of tables (**Tables 1–6**).

Institutional Abbreviations

BP, Evolutionary Studies Institute (formerly Bernard Price Institute for Palaeontological Research), University of the Witwatersrand, Johannesburg, South Africa; GMPKU, Geological Museum of Peking University, Beijing, China; IVPP, Institute for Vertebrate Paleontology and Paleoanthropology, Beijing, China; MSNM, Museo Civico di Storia Naturale di Milano, Italy; PIMUZ, Paleontological Institute and Museum, University of Zurich, Switzerland.

Anatomical Abbreviations

a, angular; ar, articular; arc, articular condyle; cav, caudal vertebra; cBI, ceratobranchial I (cornu branchiale); cl, clavicle; co, coracoid; cof, coracoid foramen; cp, coronoid process; cv, cervical vertebra; cr, cervical rib; d, dentary; dr, dorsal rib; dv, dorsal vertebra; ec, ectopterygoid; ext. n., external naris; f, frontal; fe, femur; fi, fibula; for, foramen; g, gastral rib; hu, humerus; i. ch, internal choana; icl, interclavicle; icl. e., emargination on interclavicle; icl. f., facet for clavicle on interclavicle; icl. p., posterior process of interclavicle; il, ilium; is, ischium; j, jugal; mc,

TABLE 1 | Measurements (in mm) of the skull bones of PIMUZ T 1559.

Element	Length	Alveolar margin	Median margin	Height/Width
Premaxilla	14.78	8.66		~3
Maxilla	33.66	33.66		7.75
Frontal	20.4		16.58	4.96
Parietal	14.68		11.83	5.27
Postfrontal	8.63 (orbital margin)			5.19 (orbita to posterodorsal process)
Postorbital	7.38			–
Jugal	20.97			6.2
Squamosal	9.03			2.07 (center); 6.39 (posterior processes)
Vomer	~23.3		–	~3.1
Palatine	18.8 resp. 7.46		–	~4
Pterygoid	29.74		25.89	~2 anterior; ~4 center; ~9.5 posterior
Quadrate	7.93			–
Parasphenoid	19.62 (anterior process)			2.35 (base)
Basisphenoid	7.94			8.6 posterior; 7.55 basiptyergoid processes

TABLE 2 | Measurements (in mm) of the mandibular bones of PIMUZ T 1559.

Element	Length	Height/Width
Total length	74.6	8.9 (with coronoid); ~5.9 (at posterior alveolar margin)
Articular	–	3.52 (height)
Dentary	39.7	3.58
Splénial	43.09	2.7
Angular	24.54	2.87

TABLE 3 | Measurements (in mm) of the anterior presacral vertebrae of PIMUZ T 1559.

Vertebra	Body length (keel to keel)	Total length (pre- to post-zygapophysis)	Height (middle)	Height (posterior margin)
Axis	11.3	14.77	~12.2	~12.8
3	–	23.71	–	–
4	20.6	26.02	10.72	13.12
5	21.13	25.46	~10.6	>12
6	21.18	25.98	11.11	14.8
7	19.55	24.5	11.72	15.32
8	16.39	22.08	–	–
9	13.05	19.45	11.62	14.32

metacarpal; mx, maxilla; man, manus; o, orbit; p, parietal; par, prearticular; ph, phalanges; pof, postfrontal; pl, palatine; pmx, premaxilla; po, postorbital; proc. pmx, premaxillary process of

TABLE 4 | Measurements (in mm) of maximum lengths of the cervical ribs (cr), the first thoracic rib (dr), and the sacral ribs (sr) in PIMUZ T 1559.

Element	Length
cr3?	58.80
cr4?	63.79
cr5	54.98
cr5?	56.29
cr6	44.52
cr6?	43.94
cr7	40.75, 42.36
cr8	24.79, 23.23
dr1?	40.94
sr1	7.20 (l), 7.78 (r)
sr2	7.73 (l), 7.40 (r)

TABLE 5 | Measurements (in mm) of the forelimb bones of PIMUZ T 1559.

Element	Length	Proximal width	Distal width	Diaphyseal diameter
Humerus	48.55 (l), 50.62 (r)	5.87 (l), 5.45 (r)	13.44 (l), 13.89 (r)	4.13 (l), 4.4 (r)
Radius	– (l), 41.61 (r)	6.26 (l), 5.72 (r)	– (l), 4.64 (r)	2.56 (l), 2.28 (r)
Ulna	– (l), 40.68 (r)	~7 (l), 6.6 (r)	– (l), 4.35 (r)	2.49 (l), 2.6 (r)

l, left; r, right.

nasal; ps, parasphenoid; pt, pterygoid; pu, pubis; q, quadrate; ra, radius; rap, retroarticular process; sa, surangular; slf, supralabial foramen; sc, scapula; sp, splénial; sq, squamosal; sv, sacral vertebra; ti, tibia; ul, ulna.

RESULTS

PIMUZ T 1559 shares many osteological features (see below) with the other described *Macrocnemus* specimens (e.g., Nopcsa, 1930; Peyer, 1937; Rieppel, 1989; Li et al., 2007), thus supporting the general assignment of PIMUZ T 1559 to *Macrocnemus*.

Systematic Paleontology PROTOSAURIA Huxley, 1871 TANYSTROPHEIDAE Gervais, 1859 MACROCNUMUS Nopcsa, 1930

Diagnosis

Small lizard-like tanytropheid protosaur with slender pointed snout, moderately elongated cervical vertebrae and neck ribs, and long and slender extremities. The following diagnostic characters (unambiguous apomorphies) are taken from the analysis of Pritchard et al. (2015, p. 12), as modified by Ezcurra (2016, p. 23): “[...] anteriorly curved, “U”-shaped suture between frontal and parietal in dorsal view; posterolateral processes of the parietal strongly posterolaterally oriented; marginal teeth recurved, with posteriorly concave distal margin [...]”

Type species

M. bassanii (Nopcsa, 1930) from the Besano Formation at Besano, Italy (Monte San Giorgio; Nopcsa, 1930).

TABLE 6 | Measurements (in mm) of stylopodial and zeugopodial elements in various *Macrocnemus* specimens.

Specimen	Humerus	Radius	H/R	Femur	Tibia	T/F
Data taken from Rieppel (1989, p. 382, table 2) [PIMUZ T 4822 = field no. A/III 208]						
PIMUZ T 2472	56.2	51.8	1.08	70.4	76.2	1.08
PIMUZ T 2477	34.0	32.2	1.06	45.0	47.9	1.06
PIMUZ T 4355	53.3	51.0	1.05	65.6	72.8	1.11
PIMUZ T 4822	–	–	–	46.8	47.3	1.01
Data taken from Premru (1991, p. 54, tables 2, 3)						
MSNM BES SC111	26.0	24.4	1.07	34.3	37.9	1.10
PIMUZ T 2472	57.3	52.6	1.09	71.3	77.4	1.08
PIMUZ T 2474	47.5	45.4	1.05	–	–	–
PIMUZ T 2475	37.5	35.0	1.07	–	–	–
PIMUZ T 2476	–	–	–	72.0	72.0	1.00
PIMUZ T2477	–	–	–	45.2	48.0	1.06
PIMUZ T2815	–	–	–	75.6	79.9	1.06
PIMUZ T2816	–	–	–	34.7	38.2	1.10
PIMUZ T 4355	53.3	49.3	1.08	66.0	72.8	1.10
PIMUZ T 4822	–	–	–	47.3	45.2	0.96
Data taken from Renesto and Avanzini (2002, p. 38, table 1)						
MSNM BES SC111	–	–	–	34.5 (l)	38.0 (l)	1.10
Data taken from Li et al. (2007, p. 1604, table 2) and Jiang et al. (2011, p. 1233, Table 1)						
GMPKU-P–3001	71.0 (l)	59.5 (l)	1.19	87.5 (l)	86.0 (l)	0.98
	–	–	–	87.3 (r)	86.4 (r)	0.99
IVPP V15001	71.6	59.4	1.21	90.0 (r)	87.5 (r)	0.97
Data taken from Fraser and Furrer (2013, p. 203, table 1)						
MSNM BES SC111	–	–	–	34.27 (l)	37.82 (l)	1.10
PIMUZ T 2472	–	–	–	72.02 (l)	75.91 (l)	1.05
	–	–	–	70.00 (r)	75.83 (r)	1.08
PIMUZ T 4355	–	–	–	65.95 (r)	72.75 (r)	1.10
PIMUZ T 4822	–	–	–	46.91 (l)	45.01 (l)	0.96
PIMUZ A/III 1467	–	–	–	62.75 (l)	78.92 (l)	1.26
	–	–	–	57.94 (r)	73.28 (r)	1.26
Data (this paper) (PIMUZ T 5918 = cast of MSNM BES SC111; T 2476 = cast of destroyed Milano original “Besano II”)						
PIMUZ T 1559	50.62 (r)	41.61 (r)	1.22	–	–	–
PIMUZ T 2472	58.42 (l)	52.63 (l)	1.11	72.20 (l)	76.94 (l)	1.07
	–	–	–	69.62 (r)	76.18 (r)	1.09
PIMUZ T 2475	36.6	34.5	1.06	–	–	–
PIMUZ T 2476	–	–	–	71.71	72.39	1.01
PIMUZ T 4355	53.09 (l)	48.96 (l)	1.08	65.69 (r)	72.90 (r)	1.11
PIMUZ T 4822	–	–	–	47.25 (l)	48.34 (l)	1.02
PIMUZ T 5918	25.92 (l)	24.27 (l)	1.07	34.11 (l)	38.24 (l)	1.12
	26.69 (r)	24.46 (r)	1.09	–	–	–

l, left; r, right; Ratios are given in bold.

Included species

Macrocnemus bassanii (Nopcsa, 1930); *Macrocnemus fuyuanensis* (Li et al., 2007); *Macrocnemus obristi* (Fraser and Furrer, 2013). The different species of *Macrocnemus* have been erected mainly

based on proportional differences of limb bones, rather than on discrete anatomical characters.

Age and paleogeography

Middle Triassic (Anisian-Ladinian) of Europe and China (possibly also early Late Triassic: Jiang et al., 2011).

Note

Note that the generic name was misspelled while erecting the type species *Macrocnemus bassanii* by Nopcsa (1930), later rectified by B. Peyer (see Nopcsa, 1931; Peyer, 1931, 1937). Apomorphies and current phylogenetic framework for Tanystropheidae are given in Ezcurra (2016).

MACROCNEMUS BASSANII Nopcsa, 1930

Holotype

The holotype MSNM 14624 (cast of MSNM specimen Besano I; see Ezcurra, 2016) of *M. bassanii* is a slab and counter slab with articulated, but fragmentary and poorly preserved skeletal remains from the Besano Formation (“Grenzbitumenzone”) of Cave di Besano, Porto Ceresio, Provincia di Varese, Italy (Nopcsa, 1930). The original fossil was destroyed during WW II (Fraser and Furrer, 2013).

Referred specimens

Several specimens from the Besano Formation and one specimen from the Meride Limestone, Monte San Giorgio, Switzerland and Italy (PIMUZ and MSNM collections; listed in Rieppel, 1989, as well as in Premru, 1991 and Renesto and Avanzini, 2002).

Previous diagnosis

According to Peyer (1937) PIMUZ T 2475 specimen “Valporina, 1933” should serve as the “hypotype” [“Hypotypoid,” p. 95] of the re-described species *M. bassanii*, because of the apparent lack of diagnostic characters of the holotype MSNM 14624. According to our knowledge, an official appeal to erect PIMUZ T 2475 as neotype for *M. bassanii* has never been formulated.

Accompanying this “hypotype” specimen, the following diagnosis was originally provided both in German and in Latin (Peyer, 1937, p. 95–97): “Lizard-like saurian, finds of ca. 35–86 cm total length; probably also even larger specimens. Skull definitely with upper temporal opening framed by postorbital and squamosal, otherwise likely no complete lower temporal arcade. Snout moderately elongated, very low, formed by the small premaxilla and the larger, triangular maxilla. The anterior rim of the orbit is situated about mid-length of the skull. Squamosal with four processes, *Sphenodon*-like. Nasals, frontals and parietals separated by median suture. Frontal forms orbital rim dorsally for short distance. Teeth of marginal jaw elements pointy-conical and slightly recumbent. Premaxilla with ca. 11, maxilla with ca. 25, dentary with ca. 30 teeth; vomers, palatines and pterygoids also tooth-bearing. Mandibles elongated, without extending (or prominent) coronoid process. Vomers paired and elongated, pterygoids caudally likely separated by wide gap, basisphenoid small with long tapering rostrum. Vertebrae amphicoelous. Ca. 7 cervical-, ca. 17 thoracic-, 2 sacral-, and ca 40–50 caudal vertebrae. Cervical vertebrae *Protosaurus*-like, elongated, the longest ones being more than twice as long as

the trunk vertebrae [=Rumpfwirbel]. Neural spines of moderate height, of similar length from the head to the beginning of the tail, thus forming an almost continuous ossified ridge line [=verknöcherte Firstlinie]. Sacrals and anterior caudal vertebrae shorter than the more posterior caudals. Cervicals with indistinct intercentra, in the anterior part of the tail region intervertebral situated hemapophyses whose legs are dorsally connected by a bar [=Querspange]. Cervical ribs elongated bony rods, shorter than in *Tanystropheus*, *Protorosaurus*-like. Anterior-most thoracic ribs dichoccephalic, all other monocephalic. Both pairs of sacral ribs broadened in lizard-like fashion [=lacertilierartig]; anterior caudal vertebrae with extending lateral processes which should correspond to the fused caudal ribs of lacertilians. Pectoral girdle with large interclavicle and curved clavicles. Scapulae dorsally strongly expanded. Coracoids rhynchocephalian-like, with innervation foramen, but without fenestrae. Long bones of both extremities likely hollow. Humerus slender, *Araeoscelis*-like, but without the ect- or entepicondylar foramen. Radius and ulna approximately of similar length to the humerus. Carpus in the present small specimens with fewer ossified elements compared to *Protorosaurus* and *Araeoscelis*. Phalangeal formula of the manus 2 3 4 5 3. Pelvic girdle very similar to *Tanystropheus*; ilium with dorsal blade, pubis with obturator foramen, ischium medially fan-shaped. Pronounced puboischiadic foramen. Femur straight, longer than humerus. Tibia and fibula of same length of slightly longer than femur, straight. Spatium interossum narrow. Tarsus with five ossified elements. Metatarsal IV distinctly longer, the marginal metatarsals short, metatarsal V bent [=gekrümmt]. Phalangeal formula of the pes 2 3 4 5 4. Gastral armor well-developed, each of its struts [=Querspangen] consisting of an unpaired median element and one inner and one outer lateral element on each side. From the Grenzbitumen-horizon [=Besano Formation] of the Anisian stage and the lower part of the Ladinian stage of the Triassic.”

Emended diagnosis

Recently, the following emended diagnosis for *M. bassanii* was provided (Ezcurra, 2016, p.23): “Small tanystropheid that differs from other archosauromorphs in the following combination of features: anteriorly curved, “U”-shaped suture between frontal and parietal in dorsal view; posterolateral processes of the parietal strongly posterolaterally oriented; marginal teeth recurved, with posteriorly concave distal margin; 24 presacral vertebrae; humerus <10% longer than radius; and tibia and fibula at least 20% longer than femur. This diagnosis is composed of the synapomorphies of the genus *Macrocnemus* found by Pritchard et al. (2015) and the differences reported by Li et al. (2007) and Fraser and Furrer (2013) between *M. bassanii* and *M. fuyuanensis* and *M. obristi*, respectively.”

Comments

This diagnosis, however, is flawed on the species level because (1) most of the listed morphological characters pertain to the generic level (which is already expressed in the last sentence of the diagnosis), in accordance to the generic diagnosis of *Macrocnemus* by Pritchard et al. (2015, p. 12, see above), (2) the number of presacrals does not allow separation between all three

Macrocnemus species (e.g., MSNM BES SC111 of *M. bassanii* has 25 presacrals, see discussion in Jiang et al., 2011), (3) “humerus <10% longer than radius” characterizes only *M. fuyuanensis*, and (4) “tibia and fibula at least 20% longer than femur” is not diagnostic for *M. bassanii*, but is the one diagnostic character of *M. obristi* (sensu Fraser and Furrer, 2013). We therefore propose that the diagnosis for *M. bassanii* should be emended to the following: Species of *Macrocnemus* with robust limb elements, only slightly longer humerus than radius (up to 11%), and only slightly longer tibia and fibula than femur (up to 12%).

MACROCNEMUS OBRISTI Fraser and Furrer, 2013

Holotype

Specimen PIMUZ A/III 1467, posterior postcranial remains comprising the pelvic region, the posterior extremities and the completely articulated tail, from the lower Ladinian of the Prosanto Formation, Ducaunfurgga, Davos, Canton Graubünden in south-eastern Switzerland.

Referred specimen

PIMUZ A/III 722, the only referred specimen, consists of an isolated right tarsus. It was also recovered from the lower Ladinian of the Prosanto Formation, west of the mountain Gletscher Ducan, southwest of the type locality.

Diagnosis

The following diagnosis was provided in the original species description (Fraser and Furrer, 2013, p. 200): “Species of *Macrocnemus* with gracile limb elements and a tibia and fibula at least 20% longer than the femur.”

MACROCNEMUS FUYUANENSIS Li, Zhao and Wang, 2007

Holotype

IVPP V15001, a nearly complete and mostly articulated skeleton from the Ladinian Zhuganpo Member, Falang Formation, Huabi of Fuyuan, Yunnan Province, south-western China.

Referred specimen

GMPKU-P-3001, an almost complete and overall articulated skeleton missing most of the tail, also from the same strata and locality of the holotype specimen.

Diagnosis

Species of *Macrocnemus* with humerus considerably longer (around 20%) than the radius.

MACROCNEMUS AFF. M. FUYUANENSIS Li, Zhao and Wang, 2007

Referred specimen

PIMUZ T 1559, a well-preserved, but mostly disarticulated skeleton from the upper Besano Formation (upper “Grenzbitumenzone,” bed no. 139), late Anisian, from the Mirigioli/point 902 locality, near Meride, Monte San Giorgio, Canton Ticino, Switzerland. Because of the lack of the observability of the interclavicles in the described Chinese specimens IVPP V15001 and GMPKU-P-3001, we opt to tentatively refer PIMUZ T 1559 to *M. aff. M. fuyuanensis* herein.

PIMUZ T 1559 represents a smaller individual in comparison to IVPP V15001 and GMPKU-P-3001, and the humerus of the European specimen is about 30% shorter than the humeri of the Chinese specimens.

Comments

The species of *Macrocnemus* has a humerus considerably longer (around 20%) than the radius and its affinity to *M. fuyuanensis* relies only on similar forelimb proportions. At the same time, PIMUZ T 1559 ultimately might turn out to be a new species, but this can only be verified by a thorough revision of all European and Chinese *Macrocnemus* specimens in the future. It differs from *M. bassanii* in having an interclavicle with wide wing-like processes and laterally pointed tips, circular emarginations on the posterior margins of the wing-like processes, smooth ventral bone surface, an anterior rod-like processes extending from a common base and enclosing a narrow V-shaped median notch, a fusiform caudal process expanded in mid-shaft region and with rounded posterior tip, with the caudal process being short, constituting about half of the total length of the bone. Unfortunately, the Chinese specimens of *M. fuyuanensis* do not show clear interclavicles that could be facilitated for comparison. PIMUZ T 1559 also differs from *M. obristi* in having generally more robust limb and axial elements.

Osteological Description

PIMUZ T 1559 shares many osteological features in the cranium and postcranium with previously described specimens, thus supporting the assignment of PIMUZ T 1559 to *Macrocnemus*. Much of the following cranial and postcranial anatomical description of PIMUZ T 1559 is thus very similar to previous descriptions given for *M. bassanii* (e.g., Nopcsa, 1930; Peyer, 1937; Kuhn-Schnyder, 1962; Rieppel and Gronowski, 1981; Premru, 1991; Renesto and Avanzini, 2002) or *M. fuyuanensis* (Li et al., 2007; Jiang et al., 2011). Nevertheless, it is important to provide osteological details herein, in order to highlight differences from previous descriptions or novelties.

Skull

The skull elements of PIMUZ T 1559 (Figures 2–4) are mostly scattered with the exception of the right premaxilla and maxilla. Measurements of skull bones are given in Table 1.

Premaxilla

The right premaxilla is preserved in right lateral view, the left one, being dislocated, in left lateral view (Figure 3). The bones show seven and eight monocuspid recurved teeth, respectively. This represents the minimum number of premaxillary alveoli, as one or two alveoli could be present in the tip of the bone that is not visible in lateral view. The premaxilla is low in shape and craniocaudally elongated. From the rounded snout tip the dorsal margin extends almost in parallel with the alveolar border. A thin maxillary process extends the dorsal margin posteriorly, so that the premaxilla articulates with the maxilla in a slightly bowed suture. In MSNM BES SC111, the three anterior-most teeth (nine to eleven in total) in the premaxilla were noted to be enlarged (Premru, 1991), a feature that could not be found in

PIMUZ T 1559. The reports of 13 premaxillary teeth in PIMUZ T 2472 (Kuhn-Schnyder, 1962) and 11–12 in GMPKU-P-3001 appear to be slightly too high because only nine teeth can be unambiguously assigned to the right premaxilla in PIMUZ T 2472 and 9–10 to the right premaxilla in GMPKU-P-3001. In the latter specimen the posterior extend of the premaxilla is considered here to have been misidentified by Jiang et al. (2011), which might be the cause for the slightly higher tooth counts.

Maxilla

The maxilla is essentially of a low, broad triangular shape in PIMUZ T 1559. The anterior point is blunt and receives the maxillary process of the premaxilla dorsally. In continuation of the process of the premaxilla, the anterior maxillary border rises slightly dorsally in a straight line up to a rounded ascending dorsal process, which lies at about mid-length of the maxilla from anterior to posterior. The posterior outline then forms a deep concavity immediately below the dorsal process before it slopes back to the pointed posterior jugal process of the maxilla. Just dorsal to the tooth row, an alveolar row of small circular maxillary foramina is present. A total of 24 teeth could be counted in PIMUZ T1559, but there is room for additional empty alveoli in the posterior parts of the maxillae. Although an exact maxillary alveolar count cannot be given in this specimen, around 30 tooth positions seem plausible if the reduction in size of the posterior teeth is taken into account (e.g., Renesto and Avanzini, 2002). As such the number of maxillary teeth in PIMUZ T 1559 is similar to previous tooth counts presented for specimens of *M. bassanii* [e.g., PIMUZ T 2475: 25 (Peyer, 1937); PIMUZ T 2472: 24–25 (Kuhn-Schnyder, 1962); MSNM BES Sc111: ca. 35 teeth (Premru, 1991), 34–35 according to Renesto and Avanzini, 2002] and *M. fuyuanensis* (GMPKU-P-3001: 27 according to Jiang et al., 2011, Fig. 2, p. 1231; 36 if all tooth positions are counted).

Nasal

A bone with a broad plate-like expansion supported by two parallel extending thickened struts, as well as a slender non-tapering process, with a marginal thickened ridge was identified as the left nasal in ventral view in PIMUZ T 1559 (Figure 4). The thickened struts are interpreted to extend ventrally, thus providing support for the posterior plate-like expansion (thus the element would be the left nasal seen in ventral view). The non-tapering process represents an elongated premaxillary process, constituting the dorsal margin of the external naris. The marginal thickened ridge of the process is interpreted to articulate medially with the process of the adjacent nasal. Close by, another bone fragment with a broad plate-like expansion displayed could be the posterior part of the right nasal in ventral view. The bone has only a short process exposed, which seems to continue into the sediment below the right pterygoid. In this case, the plate-like part of the fragment does not preserve the ventrally expanded struts visible in the left nasal. Kuhn-Schnyder (1962) was unable to identify the nasals in PIMUZ T 2472, but in his drawing of the skull (Kuhn-Schnyder, 1962: Figure 1) at least one unidentified bone with a broad plate-like end and an elongated process is indicated (between the frontals and the premaxillae) that resembles the bone identified as a nasal in PIMUZ T 1559.



FIGURE 3 | Photographs of selected skull elements of PIMUZ T 1559. **(A)** Left premaxilla in lateral view; **(B)** right premaxilla, maxilla, and dentary in lateral view; **(C)** complete left lower mandible in lateral view; **(D)** vomer in ventral view; **(E)** basisphenoid in ventral view; **(F)** palatine in ventral view; **(G,H)** pterygoids in ventral view; **(I)** right jugal in lateral view; **(J)** left jugal in lateral view with white outline indicated; **(K)** nasal and possible left ectopterygoid with white outline indicated; **(L)** posterior portion of right lower mandible in lateral view.

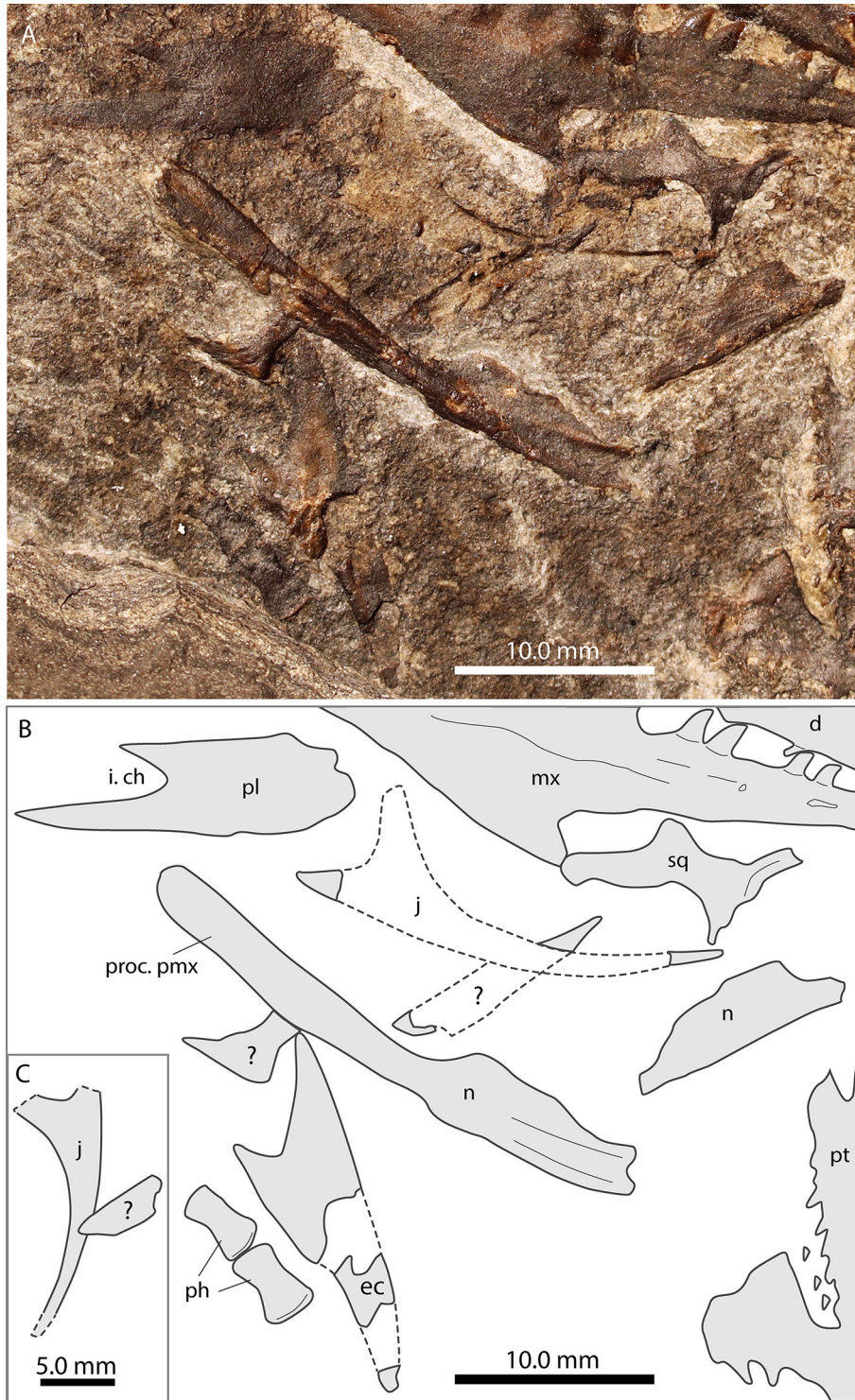


FIGURE 4 | Focus on the nasals and the jugal of PIMUZ T 1559. **(A)** Photograph; **(B)** interpretative drawing. Note long premaxillary process of nasal.

T 4822 and PIMUZ T 2472 (Peyer, 1937; Kuhn-Schnyder, 1962) could not be identified with confidence in PIMUZ T 1559.

Frontal

In PIMUZ T 1559, the paired frontals separated when the skull fell apart. Both frontals are visible in dorsal view. The right dorsal

is completely exposed, whereas the posterior-most portion of the left one is hidden by matrix (**Figure 2**). The frontals have a flat dorsal surface. The medial suture between the two bones is straight in PIMUZ T 1559 and in PIMUZ T 2472. Anteriorly the bones have a rounded shape that is delimited laterally by a narrow constriction where the bone is about three fourth of the width of the anterior part. Behind the constriction the bone becomes gradually larger again and ends in a sharp posterolateral tip. In PIMUZ T 4822, the frontal is of similar shape, but the contact between the nasal and the frontal is clearly visible as a broadly wavy suture.

Parietal

The parietals are both preserved in PIMUZ T 1559, with the left and right one each lying in close proximity but not in articulation with the left and right frontal, respectively. The parietals are twice as long as wide and with flat rhomboid outlines. If re-assembled, the anterior margin of the paired parietals would form an obtuse-angled point that would insert between the posterolateral processes of the two frontals, as has been shown for example in PIMUZ T 2472 (Kuhn-Schnyder, 1962; note that these bones are preserved in ventral view in that specimen). The preservation of GMPKU-P-3001 does not allow for an unambiguous reconstruction of the skull roof in this respect. The posterior part of the median border, as well as the whole posterior margin of the parietal, is reinforced by a ventral projection in PIMUZ T 2472. This projection extends laterally beyond the width of the bone plate.

Postfrontal

A pair of elements are interpreted as postfrontals in PIMUZ T 1559 based on comparison with MSNM BES SC111 (Premru, 1991) and GMPKU-P-3001 (Jiang et al., 2011). It is a small triangular element, with the longest edge being concave and forming the posterior dorsal margin of the orbit. The anterior and ventral processes are slightly blunt. The dorsal margin is straight and ends in a small pointed process. There is a distinct ridge projecting from the ventral process upwards.

Postorbital

Two bones, each bearing three processes are identified as postorbitals in PIMUZ T 1559. A straight process ending in a long point is likely the ventral/jugal process. The posterior/squamosal process is almost at a right angle to the jugal process and shorter, curves slightly ventrally and ends in a blunt tip. The anterodorsal process is short. In PIMUZ T 2472 the bone is visible from the inner, medial side and reveals a slightly blunt dorsal process. In that element, the straight upper end forms the base of a tiny triangular area with a point ending in a medially facing small keel along the process; this area certainly overlapped the postfrontal laterally.

Jugal

Both jugals are identifiable in PIMUZ T 1559. One is largely preserved on a separate small counter-slab that was removed during preparation, but the posterior-most tip of the posterior process is still present with the impression of the bone on the main slab. The other jugal is partially hidden by the left ilium

and its dorsal process has partially broken off. In contrast, the posterior border of the jugal is only incompletely preserved or broken off in PIMUZ T 2472 (Kuhn-Schnyder, 1962), MSNM BES SC111 (Premru, 1991; Renesto and Avanzini, 2002) and specimens PIMUZ T 4822 and PIMUZ T 4355. Similar to the jugal shown and described in GMPKU-P-3001 (Jiang et al., 2011), it is an elongate triangular bone with three processes. The longest, the anterior maxillary process, is rather thin and contributes to the ventral orbital margin. Posteriorly the bone expands into two broader processes: a dorsal postorbital process which slopes steeply upwards to meet the ventral process of the postorbital and a posterior process that extends the slightly ventral convex margin toward, but not reaching, the quadrate.

Squamosal

Only one of the squamosals could be identified in PIMUZ T 1559, based on the peculiar shape of the bone which is slightly elongated axially and possesses four distinct processes (e.g., PIMUZ T 2475: Peyer, 1937; PIMUZ T 2472: Kuhn-Schnyder, 1962; GMPKU-P-3001: Jiang et al., 2011). The longest and broadest process faces anteriorly and probably joined the posterior process of the postorbital to form the ventral margin of the upper temporal fenestra. Ventral to the first, a second, shorter process extends anteroventrally. Posteriorly two thin processes extend dorsally and posteroventrally respectively. In PIMUZ T 2472 the medial side of the squamosal reveals a concave articulation socket, probably for the articulation with the quadrate.

Vomer

A long and thin bone with at least one distinct tooth row with about 18 teeth and a side-row (and possibly a third more laterally situated row) is interpreted as a vomer in PIMUZ T 1559. Because it is not entirely prepared out of the sediment, its exact shape cannot be determined and most of the teeth remain obscured, but the round cross-sections of some broken-off teeth are visible. In the specimens PIMUZ T 2476 and PIMUZ T 2477 studied by Peyer (1937; see also Kuhn-Schnyder, 1962) a row of small teeth extends the full length of the bone, flanked by a more lateral parallel row in the posterior part of the vomer.

Palatine

In PIMUZ T 1559, one of the palatines is well-preserved, whereas the other is flattened and incomplete. The palatine is an elongated element, over four times longer than wide. A lateral row of five teeth could be counted. The medial border is straight, the posterior border gently convex and has few teeth along the posterior part. The lateral border is shorter, extending into a broad, short maxillary process with a thickened ridge extending in parallel to the long axis of the main tooth-bearing ramus. The anterior border is concave, forming the posterior and posteromedial rim of the internal choana.

Pterygoid

About one and a half times longer than the palatine, the pterygoid consists of a very long bone plate, both in PIMUZ T 1559 and in other specimens of *Macrocnemus* (e.g., Peyer, 1937; Li et al., 2007). In PIMUZ T 1559, the left pterygoid is situated close to

the ilia of the pelvic girdle, the right one close to the first sacral vertebra (Figure 2). The pterygoid shape appears to be triangular with a very long, straight medial margin. The anterior tip is very thin, while progressing posteriorly the bone expands laterally. It is unclear whether it expands continuously (i.e., if the lateral palatal ramus is straight) or if it expands in two to three marked steps. A row of 16 teeth projects along the median margin. Laterally, two close parallel rows of 11 teeth form a staggered line. Lateral and parallel to the median row, a row of 12 teeth extends from the anterior margin of the pterygoid to end halfway back along the element. Near the anterior tip of the pterygoid another three to four teeth form a smaller intercalated row.

Toward the posterior medial corner of the pterygoid a small round process may have formed part of the articulation between an epipterygoid (not unequivocally identified in PIMUZ T 1559) and the basiptyergoid process. Lateral to this, the quadrate ramus extends backwards as a small slender process. Only a caudally oriented thin rod is visible on the surface, but since the quadrate ramus is a vertical rather than horizontal structure it probably extends into the sediment. Lateral to this, on the posterior lateral margin, the bone expands in a wing-like pterygoid flange.

Ectopterygoid

In PIMUZ T 1559, a broad elongated bone with a tapering anterior end and a forked posterior margin is tentatively identified as the left ectopterygoid in dorsal view (Figure 4). As such the longer, slightly convex margin constitutes the lateral margin for articulation with the maxilla and the jugal, whereas the shorter part of the fork serves as the articulation with the pterygoid.

Quadrate

In PIMUZ T 1559 a blocky bone close to the dorsal side of the left maxilla was identified as the right quadrate displayed in anterior view. It bears a stout ventral condylar expansion (facing the left maxilla; the ventral condylar facet itself is still hidden by matrix), a concave medial margin with a strong anteromedial keel and a distally straight lateral margin expanding dorsolaterally into a plate-like extension. The plate and the main body of the quadrate are preserved at an obtuse angle to each other. The dorsal margin of the quadrate is flat to slightly concave where it likely articulated with the squamosal. It is thus very similar to the quadrate of PIMUZ T 2472, which has a large condylar area for the articulation with the mandible, an area described as “saddle-formed” by Kuhn-Schnyder (1962) and Premru (1991).

Para-basisphenoid

The parasphenoid seems to be fused with the basisphenoid in PIMUZ T 1559 (element seen in ventral view), and it conforms to the description of the element in PIMUZ T 2472 given previously (Kuhn-Schnyder, 1962). In both specimens, the triangular-shaped para-basisphenoid has a long tapering cultriform process and well-developed basiptyergoid processes for articulation with the pterygoid. According to Rieppel and Gronowski (1981) the well-developed basiptyergoid processes are indicative of a movable palatobasal articulation. This

in turn demonstrates a metakinetic skull in *Macrocnemus*, but contra Kuhn-Schnyder (1962) and Wild (1973), not streptostylic.

Stapes

Although, some rod-like elements are present in the skull region in PIMUZ T 1559, a stapes could not be unequivocally identified. A rather straight rod-like bone with a slightly broadened foot-plate was described as the epipterygoid based on the X-ray image in the posterior part of the skull of PIMUZ T 2472 (Kuhn-Schnyder, 1962), but the identification was very tentative. Given that its morphology is very similar to the rod-like bone identified as a stapes in *Tanystropheus* (Wild, 1973; Figure 1) it might also represent the stapes in PIMUZ T 2472.

Cranial openings

The disarticulated skull bones in PIMUZ T 1559 render it impossible to make any definitive statements regarding the nature of the cranial openings in this specimen. A small ventral notch might be present bounded anteriorly and dorsally by the premaxilla and posteriorly by the maxilla. A foramen in a similar position was also previously indicated in MSNM BES SC111 but misidentified as the “naris?” (Premru, 1991); whereas no foramen was indicated by Renesto and Avanzini (2002). PIMUZ T 4822, which has a well-articulated left premaxilla and maxilla, exhibits only a very tiny ventral notch between the alveolar margins of the bones.

All skulls of the European specimens are more or less displayed in lateral view. These specimens do not show undisturbed skull roofs, so that the clear identification of cranial openings is hampered. In PIMUZ T 2472 and PIMUZ T 4822 the round orbits (16.9 and 11.6 mm in diameter) are the only skull openings completely encircled by bones. Based on the morphology of the posterior skull roof bones, Kuhn-Schnyder (1962) inferred that the upper temporal fenestra was framed by the parietal, postfrontal, postorbital, and the squamosal. This was corroborated by other specimens as well (Rieppel and Gronowski, 1981; Jiang et al., 2011). Indeed, GMPKU-P-3001 is the specimen whose skull is exposed in dorsolateral view, displaying most of the skull roof still in articulation. The lower temporal fenestra, on the other hand, remained open in *Macrocnemus*. Based on the X-ray and the prepared specimen PIMUZ T 2472, Kuhn-Schnyder (1962:116) was unsure about the presence of a posterior lower process of the jugal. Nevertheless, even if a short process had been present, it would not have reached the quadrate (or possibly a quadratojugal not identified in PIMUZ T 1559), which was confirmed later also in PIMUZ T 4822 (Rieppel and Gronowski, 1981). The posterior process of the jugal is visible in PIMUZ T 1559, longer than described in PIMUZ T 4822, but similar in size to that of GMPKU-P-3001 (in which it is partially hidden by the right mandible), ventrally framing the anterior part of the lower temporal emargination. There is no evidence of any additional pre- or postorbital openings in PIMUZ T 1559 or any of the other specimens studied.

Mandible

In PIMUZ T 1559 the mandibular rami are still in contact in the symphyseal area and both are preserved in lateral view (**Figure 3**). The left ramus is mostly articulated, whereas in the right one the posterior portion of the mandible (surangular, articular and coronoid) has been separated from the anterior portion (comprising the dentary, splenial, and angular, as well as a sliver of the prearticular). Measurements of mandibular bones are given in **Table 2**. Together with IVPP V15001, the mandibular rami of PIMUZ T 1559 are among the most complete and best preserved remains known for *Macrocnemus*. The exposed right adductor fossa in PIMUZ T 2472 is 16.4 mm long and ~4 mm high.

Dentary

In all specimens studied, the dentary is a large, elongate tooth-bearing element, with a rounded anterior tip and a straight alveolar margin extends mostly parallel to the ventral edge of the dentary. The dentary tapers posterodorsally. In PIMUZ T 1559 the tapering part overlies the articular and surangular in lateral view and the splenial in ventral view. This is in accordance with the condition described in MSNM BES SC111 (Premru, 1991; Renesto and Avanzini, 2002), but in contrast to the description of a posteriorly bifurcated dentary in GMPKU-P-3001 (Jiang et al., 2011). The proposed bifurcation, however, results from the obscured and thus misinterpreted suture between the dentary and the splenial as is clearly visible in PIMUZ T 1559 and IVPP V15001. The posterior morphology of the dentary is unclear in PIMUZ T 2472 (Kuhn-Schnyder, 1962; VPJ pers. obs.). There are a few foramina along the anterior lateral side of the dentary in PIMUZ T 1559. The shallow “groove” on the posterolateral side of the dentary seen in PIMUZ T 1559 is interpreted as a taphonomic compaction of the bone just below the ventral extent of the alveolar row.

Splenial

With the exception of the anterior dentary tip the splenial underlies the dentary ventrally along its entire length in PIMUZ T 1559 (as is the case in IVPP V15001; but not described by Li et al., 2007 and Jiang et al., 2011). It forms a strong transversally reinforced bar. The ventral side is straight, almost parallel to the alveolar border of the dentary. It has a long posteroventral tapering process and the posterior part is dorsolaterally concave, likely to accommodate the Meckel's cartilage.

Angular

The angular is an elongate, flat bone, which is slightly curved dorsally in the mid part of the bone. The anterior part inserts in an acute angle between dentary and splenial, whereas most of the angular overlaps the surangular and/or the coronoid in lateral view. Ventrolaterally, it articulates with the prearticular. The posterior aspect of the angular is not well-preserved in the other specimens studied (compare to Kuhn-Schnyder, 1962; Premru, 1991; Renesto and Avanzini, 2002; Jiang et al., 2011).

Surangular

In both mandibles the surangular is still in contact with the articular and the coronoid. The left surangular is broken anteriorly where it would have articulated as a wedge with the posterior tip of the dentary dorsally and the splenial ventrally. The right surangular is well-preserved and completely visible. It is of general elongated shape, articulating ventrally with (and being partially overlain by) the angular, posteroventrally with the prearticular and posteriorly with the articular. Approximately at the midst of the surangular, the coronoid process is visible in lateral view in PIMUZ T1559, as the straight dorsal border of the surangular overlies most of the coronoid. The surangular is not well-preserved in PIMUZ T 2472.

Coronoid

The coronoid is a bone of uncertain extent in PIMUZ T 1559 bearing a small but distinct coronoid process. In medial view, as seen in PIMUZ T 2472, it has an anteroventrally inclined suture with the dentary anteriorly and with the surangular posteriorly.

Prearticular

The prearticular is also of uncertain shape but appears to be elongated and sliver-like in PIMUZ T 1559. It lies beneath the articular posteriorly and ventrally, and possibly also beneath the surangular and angular ventrally.

Articular

In PIMUZ T 1559 the articulars, both visible in lateral view, appear as small bones at the posterolateral side of the mandibles, posterior to the surangular and overlying the prearticular. The articular is slightly elongated axially, with straight, parallel ventral and dorsal borders, a very short rounded posterior retroarticular process and a small anteroventral protrusion. Laterally, there is a small foramen just ventral to the condyle. In PIMUZ T 2472 both articulars are exposed in dorsal view despite the rest of the jaw being exposed in lateral view. The articulation surface is mostly flat. The dorsomedial margin of the articular forms a strong transverse ridge separating the articulation surface from the retroarticular process. Anteriorly the articular forms part of the lateral dorsal margin of the mandible above the adductor fossa and is continued by the surangular anteriorly. The retroarticular process in PIMUZ T 2472 is somewhat longer and broader than in PIMUZ T 1559. Posterodorsally a short process forms a protuberance that, according to Kuhn-Schnyder (1962), serves as an attachment point for the musculus depressor mandibulae. The posteromedial end of the retroarticular process is rounded and rugose.

Mandibular openings

No openings or fenestrations can be seen in the mandible.

Dentition

All of the marginal dentition comprises monocuspid, conical, recurved teeth, which lack any indication of carinae, serration, or labiolingual compression. The last few teeth (>14) on the dentary in PIMUZ T 1559 appear shorter and broader than the more anterior teeth. This might be a feature peculiar to PIMUZ T 1559, however, as no such trend was visible in the other

studied specimens. Because all bones with marginal dentition are visible in lateral view only, the type of attachment of the teeth to the bone in PIMUZ T 1559 can only be classified as some form of “thecodonty.” It is likely, that it is sub-thecodont as was described for MSNM BES SC111 (Renesto and Avanzini, 2002 = pleurothecodont in Premru, 1991). The teeth located on the palatal elements (e.g., on the pterygoids and vomers) are much smaller, but are also slightly recurved, similar to the ones in the pterygoid of IVPP V15001 (Li et al., 2007, Figure 2). The number of teeth varies both between two elements of a single specimen (e.g., PIMUZ T 1559) and between the specimens, but as pointed out by Premru (1991) it is not directly correlated with the size of the individuals. The numbers represented above for the respective tooth-bearing elements are thus a minimal count that reports only the teeth actually present in the fossils.

Laryngeal Apparatus

Ceratobranchial

Two long thin bony rods in PIMUZ T 1559 are interpreted as the ceratobranchial I (cornu branchiale) based on the description of the same bone identified in PIMUZ T 2472 (Kuhn-Schnyder, 1962). They are located in close proximity to the lower jaw elements and other bones from the cranium, are slightly thicker but flatter than the cervical ribs and bend at an angle of $\sim 10^\circ$ at mid-shaft (Figure 2).

Vertebral Column

The vertebral column of *M. bassanii* has been described previously in detail (Nopcsa, 1930; Peyer, 1937; Premru, 1991). For *M. fuyuanensis*, Li et al. (2007) provided vertebral counts and a description for IVPP V15001, and Jiang et al. (2011) reported on the complete presacral and sacral series of GMPKU-P-3001. For *M. obristi* only the posterior-most part of the dorsal series, the sacral region, and the complete caudal vertebral series are preserved in PIMUZ A/III 1467, thus presenting only minimal overlap with PIMUZ T 1559. Generally, the centra of the presacral vertebrae in PIMUZ T 1559 have an overall cylindrical appearance, being constricted ventrally, as well as large and amphicoelous articular surfaces (Figures 1, 4, 5). Previously, the vertebral column of PIMUZ T 2472 was not described in detail as Kuhn-Schnyder (1962) regarded the vertebral morphology as described by Peyer (1937) as adequate.

Cervical vertebrae

In PIMUZ T 1559 the almost complete but partially disarticulated cervical series including the axis is preserved (Figure 5). Only the atlas elements could not be identified as they are likely hidden by other bones. Cervicals 2–6, visible in left lateral view, are still in articulation. Cervical 7 is visible in right lateral view and cervical 8 in right ventrolateral view. The partially hidden axis appears similar to the other cervical vertebrae in shape, but is notably shorter. The following cervical vertebral centra 3–8 are strongly elongated (see Table 3). Both the dorsal and ventral sides of the cervicals are slightly concave.

The zygapophyses are also well-developed and elongated, articulating at the intervertebral joints just above the centrum, and thus leaving no visible gap for segmental nerves.

Longitudinal muscle attachment ridges are preserved on the zygapophyses. In all cervicals, the neural arches with low neural spines are expanded axially along the whole length of the vertebrae and their straight upper rim creates a continuous ridge along the neck. The neural arches are prominent and are only slightly less high than the respective cervical centra. There is a small dorsolateral lamina extending between the zygapophyses, and also a longitudinal keel extending ventrolaterally on the centra. The cervical ribs articulate anterolaterally with the vertebral centrum. The attachment sites on the centra are roughly triangular, but the shape of the attachment with the capitulum and tuberculum of the cervical ribs are not clearly visible.

In comparison, a break in the block of PIMUZ T 2472 destroyed parts of the anterior cervical vertebral column, which is visible in right lateral view. Half of the fourth vertebra is still present on one side of the break, the other side bearing mostly fragments of the third vertebra and a small vertebral centrum represents the axis. No part of the neural arch of the axis could be identified; the anterior ventral edge of the axis is beveled.

Dorsal vertebrae

The dorsal vertebrae in PIMUZ T 1559 are much shorter than the cervical vertebrae (Table 3). In most dorsals the centra are continuous with the neural arches with no apparent suture separating the two. Because the dorsals are shorter than the cervicals, the ventral sides of the former appear more strongly concave. The dorsals are amphicoelous and the articular facets are not oriented vertically but are slightly anterodorsally-posteroventrally angled. The neural spines are higher than those of the cervicals, of trapezoidal shape and with a concave anterior edge. Similar to the cervical vertebrae, the spines also form a straight, continuous dorsal ridge line over the thoracic vertebral column. Toward the posterior part of the vertebral column, the whole neural spine of the vertebral arch shifts posteriorly on the vertebra, until in the posterior-most dorsals the posterior margin of the neural spine extends even slightly past the level of the posterior tip of the postzygapophysis. The zygapophyses expand nearly equally laterally and anteroposteriorly. The transverse processes of the first few dorsal vertebrae as seen in PIMUZ T 1559 are long and broad and with flat articulation facets for the tuberculum of the dicocephalic ribs. Progressing posteriorly the transverse processes become shorter with a more circular articular surface for the monocephalic ribs and positioned toward the more anterior part of the vertebrae at mid-height between the centrum and prezygapophysis. The prezygapophysis of the last dorsal vertebra, as well as of the first sacral are strongly expanded distally and face directly upwards, slightly tilted medially.

Sacral vertebrae

The two sacral vertebrae of PIMUZ T 1559 have a similar centrum shape to the dorsal vertebrae, except that they are wider than high, especially in the second sacral (Figure 2). The first sacral is visible in anterior view with stout pedicles framing an oval shaped neural canal but lacking the neural arch; the second sacral is preserved in ventral view. The sacral ribs are sutured to the vertebral centra and not fused (best visible in the

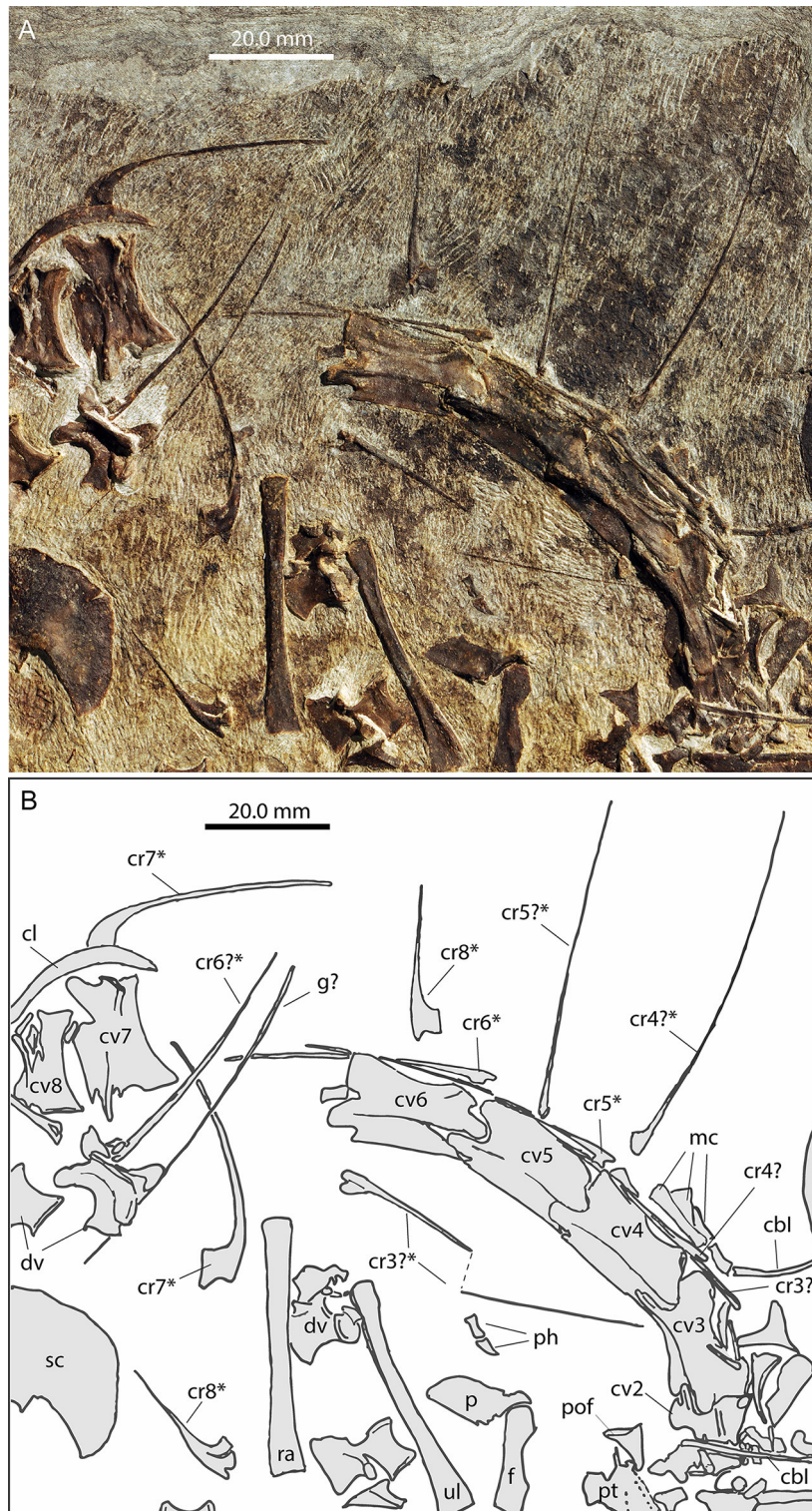


FIGURE 5 | Focus on the neck region of PIMUZ T 1559. **(A)** Photograph; **(B)** interpretative drawing. Cervical ribs that were measured (**Table 4**) are marked with an asterisk (*).

second sacral: Supplementary Figure 2). The base of the first sacral rib is robust and dorsoventrally expanded. In axial view, the rib first becomes more slender before expanding distally,

as the dorsal margin of the sacral rib remains almost straight. The distal articulation surface for the ilium is slightly tilted ventrally. The height of its articular surface with the ilium is

4.11 mm. In PIMUZ T 2472, the first sacral vertebra is visible in dorsal view, showing that the sacral rib starts as a narrow rod-like structure which distally broadens anteroposteriorly (Rieppel, 1989). The sacral rib of the second sacral in PIMUZ T 1559 is even more anteroposteriorly expanded (13.95 mm) than the first, and it also bifurcates with a slender spur-like posterior process. This posterior process is scythe-shaped with a strong posterior bar, bent laterally and with a thinner bony connection to the main part of the rib. It is unclear whether the posterior process articulated with the ilium as well. The length of the articular surface of the second sacral rib with the ilium is 8.11 mm. As seen in PIMUZ T 2472 (see also Rieppel, 1989, Figure 1) the second sacral rib overlaps the posterior margin of the first sacral rib laterally, thus enclosing a roughly oval shaped gap in between.

Caudal vertebrae

In PIMUZ T 1559 the tail is essentially lacking and only a single vertebra close to sacral vertebra 2 is present (Figure 2). Based on comparison with PIMUZ T 2472 and IVPP V15001 it is tentatively identified as the anterior-most caudal in posteroventral view. It is generally similar in shape and length to the posterior-most dorsals, with a cylindrical centrum and expanded anterior and posterior articulation facets. Dorsolaterally, the vertebra has a long blade-like transverse process, which is angled posteriorly and tapers laterally into a point. The anterior margin of the process is concavo-convex, whereas the posterior margin is straight. No hemapophyses were identified in PIMUZ T 1559.

Cervical ribs

In PIMUZ T 1559 the cervical ribs are dichococephalic with posteriorly very thin elongated rods (Figure 5). They articulate with the vertebrae at the anterior basal edge of the centrum with a distinctly separate tuberculum and capitulum. Anteriorly the ribs form a small rod-like process and posteriorly a very long and delicate process the latter spanning up to two or three intervertebral joints in length, as far as preserved. In PIMUZ T 1559 the longest preserved cervical rib (no. 4?) is 63.8 mm long. Given that the combined length of the longest cervicals (nos. 4–6) ~63 mm (see Table 4), the longest cervical rib would still span three intervertebral joints. The ribs of the posterior-most cervical vertebrae are much shorter, though the rib shaft is still straight. The capitulum and tuberculum of the shortest cervical rib (no. 8) are still separated and extend mostly parallel in the ribs of cervical 8.

Dorsal ribs

The dorsal ribs of PIMUZ T 1559 have scattered so that there is no contact with the vertebrae anymore (Figures 1, 6). According to the vertebral count and comparison with other specimens (i.e., PIMUZ T 2472; GMPKU-P-3001), a total of 34 dorsal ribs should be present, but only 22 ribs could be identified. Six of the 22 are clearly dichococephalic, with a short dorsal tuberculum and a long ventral capitulum for articulation. The presumed rib following cervical rib 8 has a longer shaft again, is slightly curved like the

other clearly dichococephalic thoracic ribs and is thought likely to have reached the sternum (although it is about 7 mm shorter than the definitive thoracic ribs).

Directly distal to the head the thoracic ribs angle strongly ventrally, but the rib shafts are more smoothly curved distally, and some show a proximodistally trending furrow along the shaft. The first definitive dichococephalic rib (interpreted to be the first or second of the thoracic series) measures 40.94 mm in length, and is thus about 1.6 times longer than the ribs of the last cervical (Table 4).

The remaining 16 ribs are either holocephalic with only a single articulation or remain partially embedded in matrix so that the second articulation is not visible. Considering the latter, it is thus possible that, as mentioned by Jiang et al. (2011), the first five vertebrae carry dichococephalic ribs. In PIMUZ T 2472 the ribs of the last few dorsal vertebrae are still in articulation. The ribs associated with the 7th to last thoracic vertebra are long and slightly curved in PIMUZ T 2472. Successive ribs are increasingly straight and short until the penultimate thoracic vertebra, which bears shorter “prong-like” ribs. The dichococephalic ribs are thus restricted to the anterior thoracic region. Those of the last dorsal vertebra are only marginally longer, but expanded distally. Otherwise the dorsal ribs follow the morphology described previously by Peyer (1937).

Pectoral Girdle

All bones of the shoulder girdle are preserved and lie isolated and disarticulated in PIMUZ T 1559 (Figures 6–8), including the interclavicle, which is also preserved more or less isolated in PIMUZ T 2475 and PIMUZ T 4355 (Figure 7).

Interclavicle

In PIMUZ T 1559 the interclavicle is visible in ventral view. It is 43.35 mm long and forms a broad triangular plate anteriorly bearing two lateral pointed wing-like processes, a slightly convex anterior margin, and a prominent caudal process. Although the tip of the right process is hidden and thus the maximum width could not be measured precisely, it is estimated to be about 35 mm (measured by doubling the length from the midline to tip of left process). A small median outgrowth projects forwards from the anterior margin. This protuberance encloses a narrow V-shaped median notch. Extending from the median protuberance and along the gently backwards sloping anterior lateral borders are clearly delimited and mediolaterally striated articular facets for the clavicles (icl. f.; Figures 7A,B). Posterior to the lateral points on the slightly concave posterolateral borders of the triangular plate, small but clearly delineated circular emarginations are present on each side (icl. e.; Figures 7A,B), which are so far unknown in the interclavicles of other *Macrocnemus* specimens. The rest of the lateral margin of the triangular plate is thin and irregular, probably due to a cartilaginous covering in the living animal as proposed by Peyer (1937) based on PIMUZ T 2475. The caudal process is fusiform with slightly convex margins (forming a thickened mid-shaft region) and a blunt tip. The caudal process contributes to approximately half of the total length of the bone. The ventral bone surface of the interclavicle is smooth.

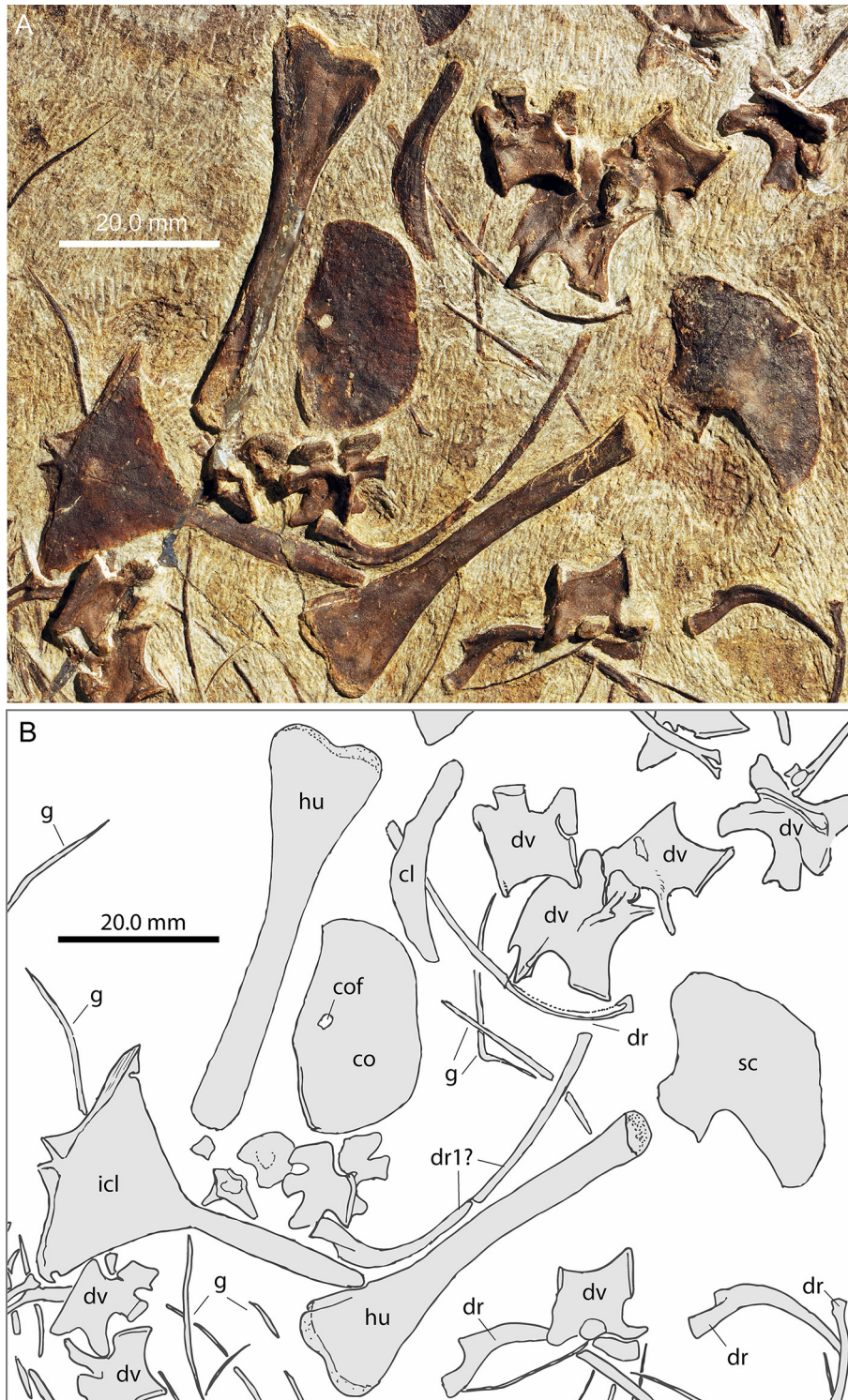


FIGURE 6 | Focus on the pectoral region of PIMUZ T 1559. **(A)** Photograph; **(B)** interpretative drawing.

The interclavicle of PIMUZ T 4355, already described in detail by Rieppel (1989) is visible in dorsal view, but because it is partially broken, the imprint of the ventral side is also

visible in the matrix (**Figures 7C,D**). It shares the same overall shape with the interclavicle of PIMUZ T 2475. Both display a reduction in lateral extent of the wing-like processes, blunted

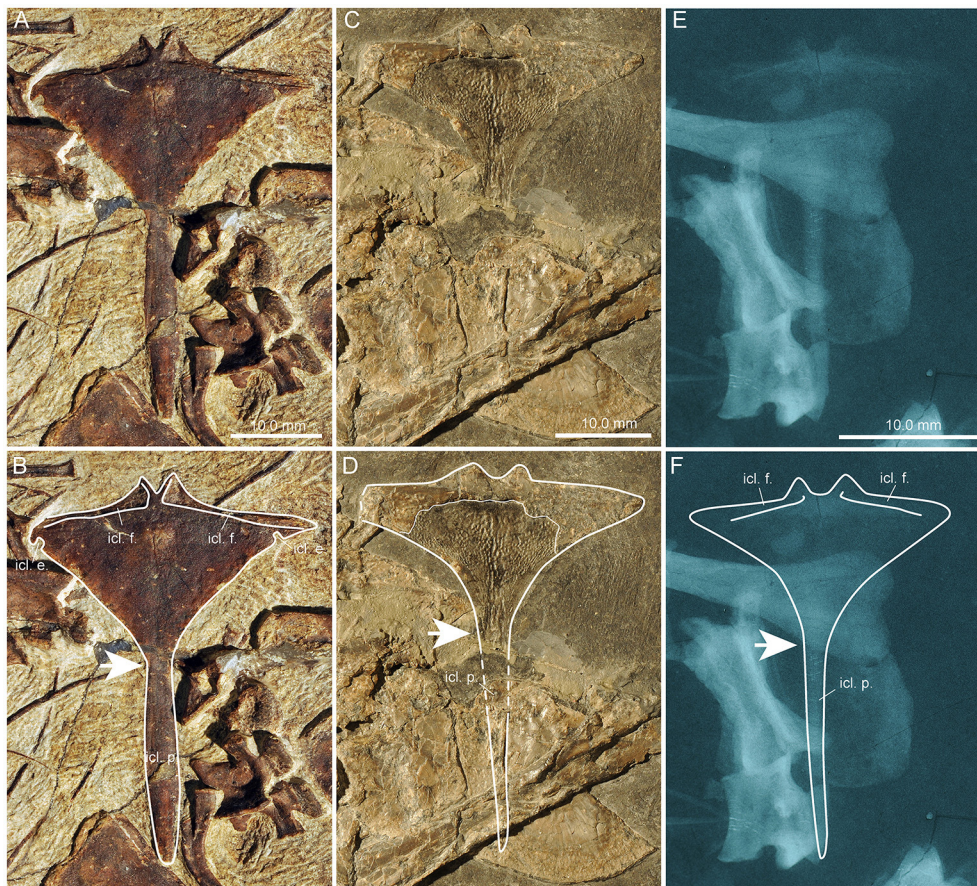


FIGURE 7 | Comparison of the interclavicles of several specimens of *Macrocnemus*. Photographs (A–D) and X-ray images (E,F) of interclavicles with interpretative drawings superimposed (B,D,F). (A,B) PIMUZ T 1559; (C,D) PIMUZ T 4355; (E,F) PIMUZ T 2475. The white arrows indicate transition from the anterior wing-like processes to the posterior process. Note the presence of small but clearly delineated circular emarginations present only at the posterior margins of the wing-like lateral processes of PIMUZ T 1559.

cranial processes enclosing a wide U-shaped median notch, and a narrow long and tapering caudal process. This specimen shows a peculiar ornamentation of the ventral bone surface (Rieppel, 1989) consisting of small tubercles and more centrally situated longitudinal ridges, not visible in specimen PIMUZ T 1559 or in the X-ray of PIMUZ T 2475.

The interclavicle of PIMUZ T 2475 (described by Peyer, 1937) is displayed in dorsal view (Figures 7E,F). It has a straighter anterior border of the anterior triangular plate than PIMUZ T 1559 and possesses rounded lateral tips. The lateral wing-like processes are somewhat slenderer than those of PIMUZ T 1559, with a straight lateral border and no emarginations just posterior to the lateral tips. Elongated articular facets for the clavicles are only discernible in X-rays of the specimen. The cranial processes are blunter, enclosing a wide U-shaped median notch in between, whereas the caudal process is long, narrows distally with straight lateral borders, and ends in a pointed tip.

Clavicle

Both clavicles are preserved in PIMUZ T 1559, the left one in anterior view is 24.52 mm long and the right one in angled

anterior view is 28.03 mm long (Figures 8A,B). The clavicle is a long curved bone with a slight torsion along the long axis of the bone. One end is slightly shorter, straight and terminates in a thickened blunt end. About mid-way along the lateral margin of the bone, near the lateral edge of the clavicle-interclavicle contact, there is a weak protuberance. The other end expands to form a broad curved blade ending in a point. The concave margin of the blade is smooth, whereas the convex side has an irregular rim and is very thin.

Scapula

Both scapulae are preserved in PIMUZ T 1559. The left scapula (29.48 mm long) is visible in lateral view and the right one (29.74 mm long) in medial view (Figures 8C,D). The scapulae of PIMUZ T 1559 are large, relatively flat plate-like elements. The scapula has a broad base with a straight ventral articulation with the coracoid and likely also extended somewhat medially. The thin blade of each scapula is separated from the base posteriorly by a constriction, with a strong posterior margin rising posteriorly and slightly dorsally, whereas the concave anterior margin frames a space with the concave anterolateral

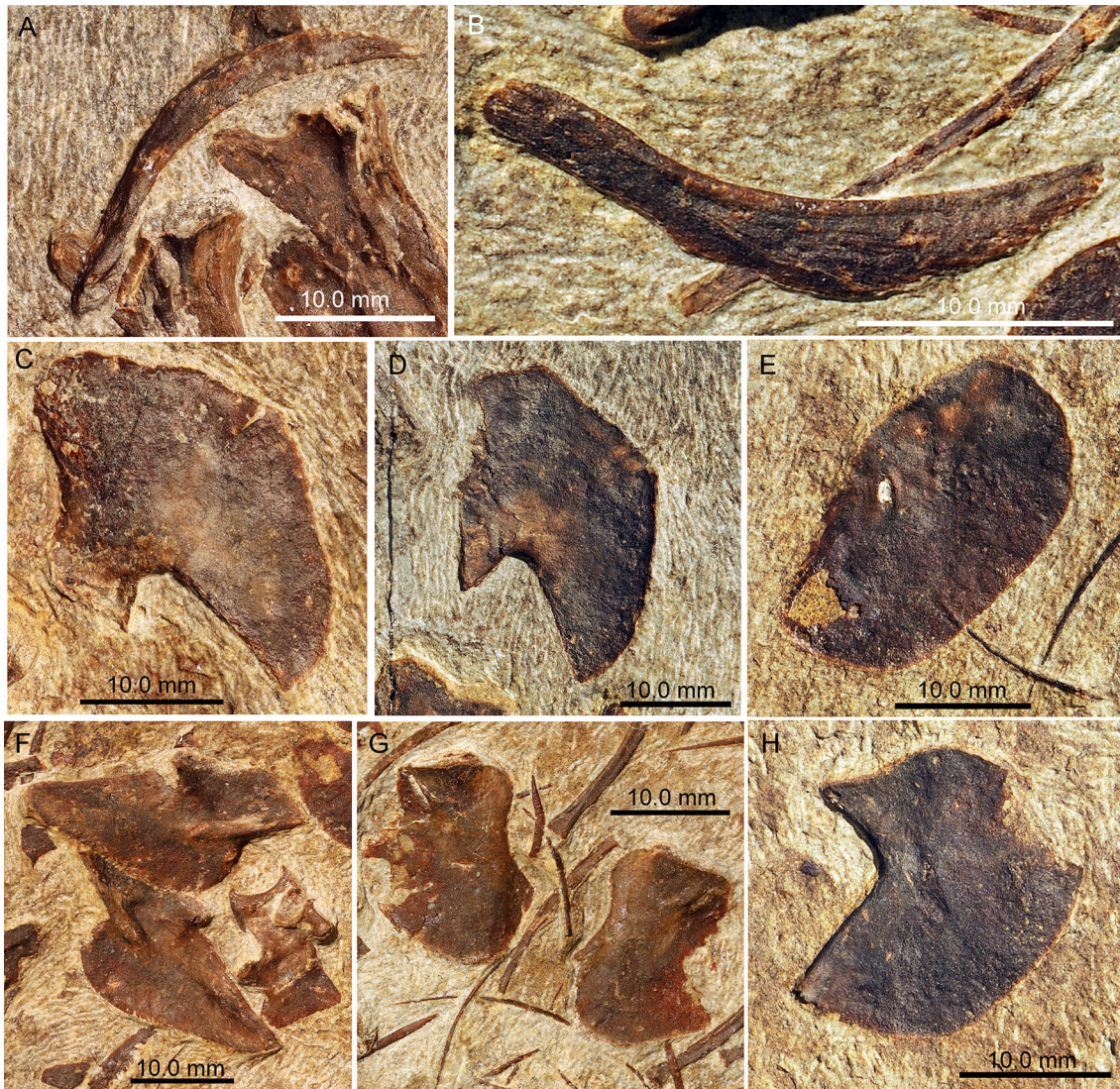


FIGURE 8 | Photographs of selected girdle elements of PIMUZ T 1559. (A) Left clavicle in anterior view; (B) right clavicle in angled anterior view; (C) left scapula in lateral view; (D) right scapula in medial view; (E) right coracoid in medial view; (F) ilia in lateral view; (G) pubes in lateral view; (H) left ischium in lateral view.

margin of the coracoid. The scapula expands almost to a half circle anteriorly where it ends at the scapulocoracoid articulation. Posteriorly on the base of the scapula in PIMUZ T 2472, just below the constriction, there is a concavity, where one might expect the supraglenoid foramen to be located.

Coracoid

The coracoid is a broad oval kidney-shaped plate in PIMUZ T 1559, and both elements are visible in medial view so that the glenoid portions are not exposed (Figures 6, 8E). The left coracoid has a maximum length of 25.02 mm, the right one 26.32 mm. Anteriorly it has a relatively longer and slightly concave edge and a shorter, also slightly concave, posterior margin. Close to the articulation with the scapula, at about the mid-length of the bone, a distinct coracoid foramen is visible.

In articulation, the scapula, with its constricted base, and the coracoid, with its concave anterolateral margin, enclose a small anterior scapulocoracoid embayment. This contrasts with the shape of the coracoid illustrated by Rieppel (1989) for PIMUZ T 2472 and described with a distinct posterior glenoid process. The data from PIMUZ T 2475 (plate 57 in Peyer, 1937); TMS pers. obs. on original X-ray stored at PIMUZ) and PIMUZ T 1559 on the other hand clearly show the oval outline of the coracoid, indicating that the putative “posterior glenoid process” in PIMUZ T2472 is an artifact caused by an underlying bone.

Forelimbs

The limbs of *Macrocnemus* are generally long and slender, and in all specimens studied the hind limbs are distinctly longer than the forelimbs. The forelimb bones of *M. bassanii* have been described

by Peyer (1937) and Premru (1991), and those of *M. fuyuanensis* by Jiang et al. (2011), so that only a brief summary is necessary here.

Humerus

Both humeri are preserved in PIMUZ T 1559 exposed in ventral view and positioned close to the elements of the pectoral girdle (Figures 1, 6). The right humerus has the same proximodistal orientation as the right radius and ulna, and the left humerus the same proximodistal orientation as the left radius and ulna, thus corroborating the assignment of the respective stylopodial and zeugopodial elements.

The humerus has a narrow straight diaphysis. In PIMUZ T 1559 the proximal portion is not expanded in ventral view, whereas the distal part is greatly expanded. The proximal expansion in the humerus, however, is strongly torqued relative to the distal end, thus likely obscuring the nature and extent of the proximal expansion. The granulated appearance of the articular surfaces is preserved and is considered to be indicative of articular cartilage once capping the bone. The deltopectoral crest is long and thin, and the pectoralis muscle attachment is situated just below the proximal articulation surface on the anterior ventral side. The distal head has two convex condyles separated by a weak intercondylar fossa. The condyles lie almost at the same level, but the ulnar condyle expands slightly farther distally than the radial one. An ectepicondylar groove is present anteriorly whereas an entepicondylar groove or foramen appears to be absent. Very fine longitudinal lines can be seen on the dorsal surface of the distal head.

Radius and ulna

Both radii and ulnae are preserved in PIMUZ T 1559 (Figures 1, 2, 5). The zeugopodial elements are long, thin bones with only slightly expanded articular surfaces (Tables 5, 6). The proximal articular surfaces appear flat in the fossil but were likely slightly concave in the living animal to receive the humeral condyles. The distal surfaces are slightly convex. The diaphysis of the radius is straight and thinnest mid-shaft. In the ulna, the diaphysis is weakly sigmoidal, the thinnest part is slightly more distal compared to the radius. The distal articular surface is smaller than the proximal one, especially in the ulna. The ulna lacks an olecranon process.

Autopodium

Four elongated elements with proximally and distally broadened epiphyseal regions and one shorter bone with a more cylindrical appearance lie close to the ventral margin of cervical vertebra 4 in PIMUZ T 1559 (Figure 5). In comparison with IVPP V15001, the longer bones are identified as metacarpals, the shorter one as a proximal phalange. Due to overlap, only the length of the single completely exposed element (12.45 mm) could be measured. In addition, a separate terminal claw and a penultimate phalanx (Figure 5) could be identified a little above cervical vertebra 4, as well as two articulated phalanges lying close to the jugal (Figure 2). In general, the elements of the autopodium do not differ in shape from other specimens of *Macrocnemus* studied. Given their position close to the neck and the skull elements, and

the lack of any identifiable hind limb elements in the specimen, they can be confidently assigned to the manus.

Pelvic Girdle

In PIMUZ T 1559, the pelvic elements have disarticulated in such a way, that the pubes and the ilia lie close to each other but the ischia have become separated from each other (Figures 1, 8). In PIMUZ T 2472 the pelvic elements are all preserved although only the posterior tip of the right ilium is preserved. The left ilium (in medial view) is still in articulation with the two sacral vertebrae while the pubes and ischia have shifted somewhat farther away from the vertebral column. PIMUZ T 2470 exhibits the left ilium and ischium preserved in articulation in medial view. To date IVPP V15001 presents the only complete and largely articulated *Macrocnemus* pelvic girdle. The right side is exposed in medial view, with the pubis and ischium just slightly separated from each other (Li et al., 2007). In GMPKU-P-3001 the pelvic elements are also mostly present, but apart from one pubis, their outlines are difficult to discern. In IVPP V15001, PIMUZ T 1559, PIMUZ T 2470, and PIMUZ T 2472, the ilium, pubis and ischium display broad acetabular processes delimited from the rest of the bone by a neck. Each of the elements contributes equally to the acetabulum. The general morphology of the pelvic bones has been described by Rieppel (1989), who also presented a revised composite reconstruction (based on PIMUZ T 2470 and PIMUZ T 2472) of the pelvic girdle in left lateral view. Our observations on PIMUZ T 1559 mostly confirm previous descriptions.

Ilium

The ilia in PIMUZ T 1559 are both preserved in lateral view (the length of the blade in left side is 22.59 mm long and the right side 22.74 mm). Immediately after the neck, the ilium enlarges into a wing-like bony plate, forming a preacetabular process with rounded anterior (i.e., semicircular) border and a postacetabular process in the form of a tapering posteriorly oriented blade. Laterally, the acetabular portion is reinforced by an anterior and a posterior strut or crest. The two struts do not meet, but the anterior strut extends through the neck to form a supraacetabular buttress. The posterior blade appears to be reinforced by a longitudinal central strut as well, though this might reflect medial structures being impressed though from the opposite side. The iliac blade displays dorsoventrally striated ornamentations where the hind limb musculature likely attached. The articular facet of the ilium for the pubis is about 6 mm long, the one for the ischium 8 mm long. In PIMUZ T 2470, PIMUZ T 2472, PIMUZ T 2475, the anterior border of the preacetabular process forms a more acute angle, whereas in IVPP V15001, the border is gently curved. The condition is inconclusive in PIMUZ T4822.

Pubis

Both pubes are visible in lateral view in PIMUZ T 1559 (Figure 8G). The pubis is the smallest and least expanded of the pelvic elements in this specimen with blade lengths of 17.67 and 17.98 mm for the left and right pubes respectively. The anterior border is only slightly concave, whereas the posterior border is more strongly concave. The obturator foramen, positioned

ventral to the acetabulum, is horizontally elongated. Together with the ischium the pubis encloses a central thyroid fenestra. The articular facet of the pubis for the ischium is 5.7 mm long.

Ischium

Both ischia are visible in lateral view (blade length of the left side is 20.96 mm, and the right side 22.65 mm) in PIMUZ T 1559 (Figures 1A, 8H). The length of the articulation between the ischium and the pubis is slightly shorter than the contact between the ischium and ilium. Both anterior and posterior margins of the ischial constriction are concave, but anteriorly the border is shorter and deeper, while posteriorly the plate extends farther and has a more smoothly concave margin. The broad ischial blade is strongly convex and its margin is obtuse-angled posteromedially.

Hind Limbs

The hind limbs are not preserved in PIMUZ T 1559.

Gastralia

The gastralia of PIMUZ T1559 are elongate, very thin elements that range from straight to weakly curved or even displaying a distinct bend with two “arms” of unequal length (Figures 1A, 2, 5, 6). The ends of the bones are simple pointed tips. They are scattered across the block. As proposed by Peyer (1937) and given the various morphologies, it is reasonable to assume that five, rather than three individual elements constitute one gastralium, with the angled ones being the medial elements, followed by the straighter ones and then the weakly curved ones laterally.

DISCUSSION

The description of the newly described specimen PIMUZ T 1559 is generally in accordance with previous descriptions of *Macrocnemus*, with the exception of the orientation of the clavicle in the pectoral girdle and the morphology of the interclavicle and the morphology and articulation of the scapulae and coracoids. PIMUZ T 1559 has the same number of cervical (8) and dorsal (17) vertebrae as specimens of *M. bassanii* (e.g., PIMUZ T 2472; MSNM BES SC111) and *M. fuyuanensis* (e.g., GMPKU-P-3001), so that vertebral counts are not useful for species designation. The forelimb proportions (H/R ratio) of PIMUZ T 1559 on the other hand clearly resemble those of *M. fuyuanensis* from China and not those of the *M. bassanii* specimens from Monte San Giorgio (see below). In addition, based on PIMUZ T 1559 and re-evaluation of the other *Macrocnemus* specimens from PIMUZ, a new reconstruction of the pectoral girdle of *Macrocnemus* is proposed. Finally, in addition to the ratio of the forelimb bones, we present a number of discrete osteological characters that can also be used to potentially separate *M. bassanii* from *M. fuyuanensis*.

Nasal Region

Due to preservation and preparation biases, the nasals are generally difficult to identify in many of the skulls of *Macrocnemus*. Peyer (1937) could not describe the exact shape of the nasal but expected the external narial opening to lie at

the mid-region between the tip of the snout and the anterior orbital rim. Renesto and Avanzini (2002) also favored a more posterior position in MSNM BES SC111. In the same specimen Premru (1991) misidentified a larger gap between the premaxilla and maxilla as the potential external naris. A more anteriorly situated external narial opening, together with the presence of a nasal groove allegedly similar to that of *Tanystropheus* (specimen PIMUZ T 2819) and *Dinocephalosaurus* were then proposed for the first time in GMPKU-P-3001 (Jiang et al., 2011). Accordingly in that study, the nasals were reconstructed as rather blocky, anteriorly bifurcated elements, with a broad lateral contact with the maxilla and a snout region that is mostly formed by the premaxillae (reaching the level of the anterior edge of the lacrimals, which were reconstructed as large crescent shaped bones lying mostly anterior to the prefrontals). Based on the new data of PIMUZ T 1559 (Figures 3, 4) and re-examination of PIMUZ T 2472, PIMUZ T 4355, PIMUZ T 4822, and MSNM BES SC111, we found that the interpretations of the skull pattern of the rostrum of GMPKU-P-3001, as shown by Jiang et al. (2011), and that of PIMUZ T 4822, as reconstructed by Peyer (1937) were equivocal (see Figures 9, 10 for our interpretations of the skull bone configuration in these specimens).

The premaxillae in PIMUZ T 1559, PIMUZ T 2472, PIMUZ T 4822, and MSNM BES SC111 are small, low bones with a dorsal maxillary process that is maximally as long as the anterior, main body (the tooth-bearing part) of the bone. These bones are thus not large enough to span further posteriorly than half of the snout region. Furthermore, PIMUZ T 1559, PIMUZ T 2475, PIMUZ T 4822, and MSNM BES SC111 demonstrate that the maxilla has a rising, straight anterodorsal margin but no anterodorsal process, which would accommodate the maxillary process of the premaxilla as proposed by Jiang et al. (2011), and only a very short straight to slightly concave dorsal margin for the articulation with the posterolateral margin of the plate-like posterior portion of the nasal. In these specimens, there is also no indication for the presence of a large crescent-shaped lacrimal as proposed for GMPKU-P-3001. With the smaller rectangular lacrimals, crescent-shaped prefrontals and frontals lacking long anterior processes and being restricted to the circumorbital region, together with a premaxilla that was restricted to the anterior half of the snout region, the nasals must be enlarged to cover the posterior snout region dorsally and dorsolaterally. This is achieved by a long premaxillary process extending anteromedially from the broader posterior region of the nasal. Accordingly, we reinterpret the skull of GMPKU-P-3001 to have short premaxillae as in all other specimens of *Macrocnemus*, and much longer nasals than reconstructed previously, and without an anterior bifurcation. The bifurcation indicated by Jiang et al. (2011) is reinterpreted as the plate-like posterior part of the nasal and the anterior premaxillary process being separated from each other by the external naris. The external naris thus would be elongated and tapering anteriorly, spanning from a level of the main body of the premaxilla anteriorly to half-way between the tip of the snout and the orbits posteriorly, contra Peyer (1937) who proposed a more posterior position only for the external naris and contra Jiang et al. (2011) who proposed that the external naris sits more anteriorly. The anterior

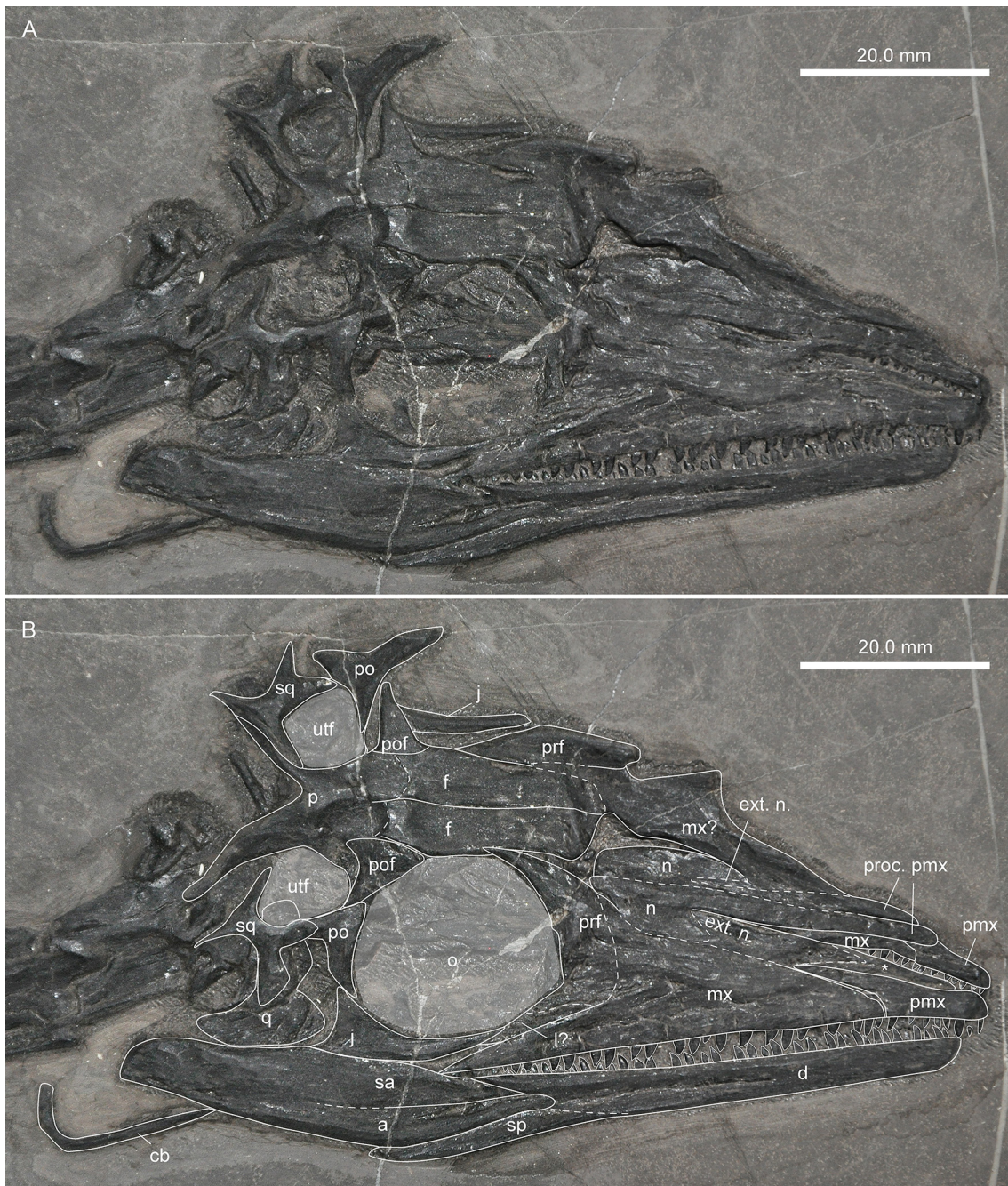


FIGURE 9 | Skull of specimen GMPKU-P-3001 of *Macrocnemus fuyuanensis*. **(A)** Photograph; **(B)** interpretative drawing superimposed. Note that the element indicated by an asterisk (*) could either be part of an exposed palate or, similarly likely, it could represent the median process of the premaxilla, which is otherwise not visible.

margin of the external naris is formed by the premaxilla; the ventral/lateral margin by the posterior process of the premaxilla and the dorsal margin of the maxilla; its dorsal/medial margin by the premaxillary process of the nasal; and its posterior rim by the plate-like expanded posterior part of the nasal.

As the external naris is extended in the skull of *Macrocnemus*, a nasal groove is not present (see **Figures 9, 10**). In comparison

with extant reptiles, the external naris would be covered largely by connective tissue forming a much smaller opening externally. The condition in *Macrocnemus* differs from that of *Dinocephalosaurus orientalis* (Li, 2003; Li et al., 2004), in which a nasal groove was first described. In the latter species, the external naris is situated far more anteriorly extending as a posterior nasal groove posteriorly on the maxilla, nasal and prefrontal.

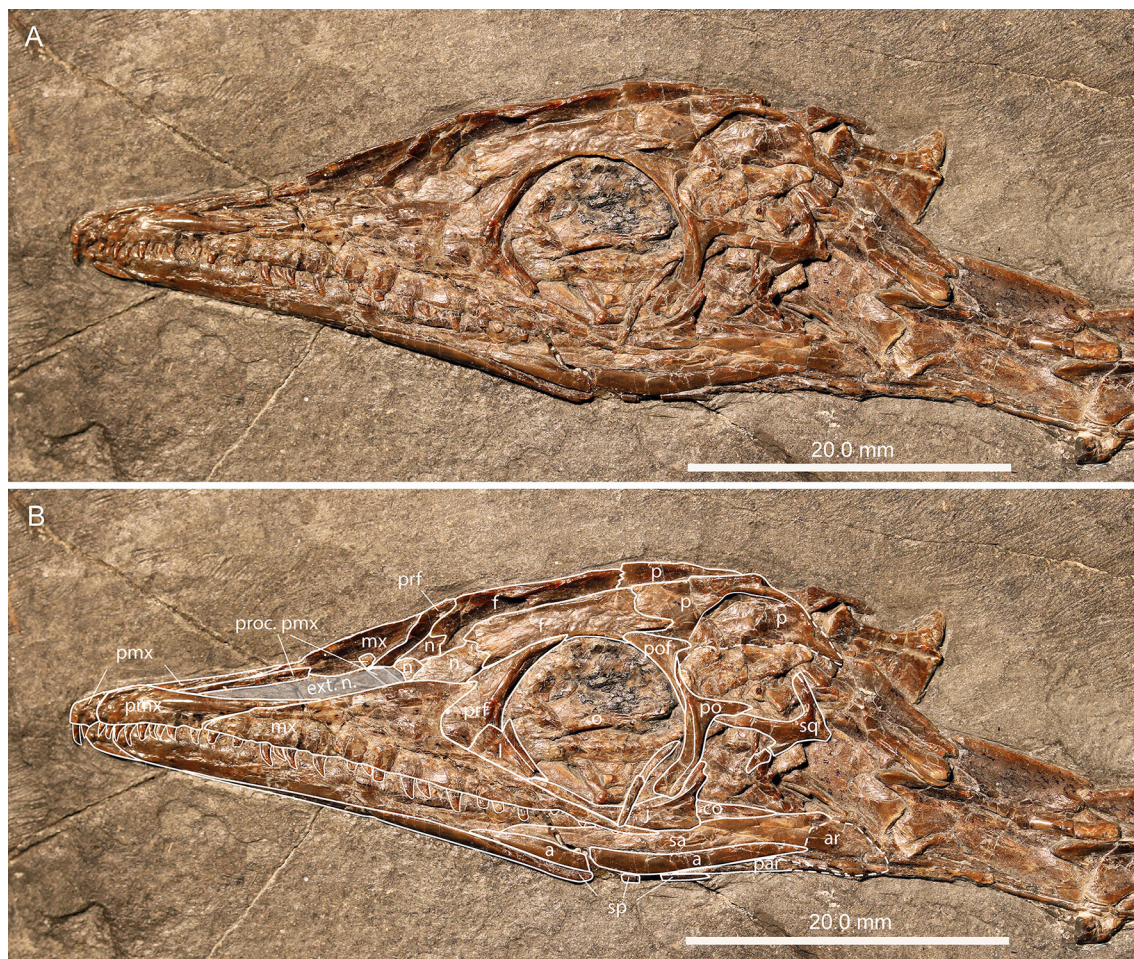


FIGURE 10 | Skull of specimen PIMUZ T 4822 of *Macrocnemus bassanii*. **(A)** Photograph; **(B)** interpretative drawing superimposed.

Premaxillary-Maxillary Contact

A putative small ventral notch was found at the suture between the anterior margin of the maxilla and the posterior tooth-bearing part of the premaxilla in PIMUZ T 1559 (Figure 3) and MSNM BES SC111, and to a lesser degree also in PIMUZ T 4822 (Figure 10) and GMPKU-P-3001. Unfortunately, the premaxillary-maxillary contact is obscured by other bones in the skull of the holotype specimen of *M. fuyuanensis* (IVPP V15001). This character is the result of an interrupted premaxillary-maxillary alveolar margin and has been scored in various previous phylogenetic studies (e.g., character 24 in Ezcurra, 2016). As noted by Ezcurra (2016), however, such a notched margin appears to reflect different conditions in different groups of animals. In the *Macrocnemus* specimens analyzed herein, the notched margin could either be a taphonomic artifact (i.e., due to a shift of the premaxilla relative to the maxilla) or a true anatomical feature. In the latter case one might speculate, whether the notch takes over the role of an anterior maxillary foramen in accommodating the anterior-most exit of the supralabial extensions of the maxillary branch of the trigeminal nerve (cranial nerve V₂), responsible also for

sensation in the nasopalatine region (Nieuwenhuys et al., 1998; see also Gottmann-Quesada and Sander, 2009 on *Protorosaurus*).

Limb Proportions

The limb proportions of PIMUZ T 2472 are congruent with those of the other described *M. bassanii* specimens, including the well-preserved and mostly articulated specimens PIMUZ T 4355 from the Besano Formation and PIMUZ T 4822 from the Cassina beds of the Meride Limestone at Monte San Giorgio (Peyer, 1937). PIMUZ T 1559, on the other hand, shows a humerus/radius ratio (humerus is 21.7% longer than the radius) which is considerably higher than in *M. bassanii* (between 5% in PIMUZ T 2474 and 11% in PIMUZ T 2472), but comparable to that of *M. fuyuanensis* (19–21%; see Table 6). Although the process of erecting species based mainly on ratios is potentially problematic, it is the one criterion that links PIMUZ T 1559 to *M. fuyuanensis*. Unfortunately the hind limbs are not preserved in PIMUZ T 1559 and therefore cannot be compared with *M. obristi* (PIMUZ A/III 1467). On the other hand, PIMUZ A/III 1467 has very slender and gracile limbs, which are at odds with the more robust forelimb elements seen in PIMUZ T 1559. Sexual dimorphism in

M. bassanii has previously been investigated by Premru (1991). In a study of four specimens she noticed that in two, all limb bones were about 10% shorter compared to the overall length of the fossil, and deemed sexual dimorphism the most likely explanation. It thus would seem unlikely that the increased length of an individual bone (the humerus in *M. fuyuanensis*; the tibia in *M. obristi*) is related to sexual dimorphism, although this aspect needs to be tested with more specimens.

In general, although measurements vary slightly between the left and right side in one individual, as well as between studies on the same specimen, ratios are consistent overall (Table 6). Previous negative or equal T/F values in PIMUZ T 4822 and PIMUZ T 2476 presented by Premru (1991) and Fraser and Furrer (2013), however, could not be reproduced; instead our tibia and femur measurements in PIMUZ T 4822 are in accordance with Rieppel (1989, i.e., in having a tibia that is longer than the femur).

Interclavicle Shape

The interclavicle of the newly referred specimen of *M. aff. M. fuyuanensis*, PIMUZ T 1559, differs from the two interclavicles known for *M. bassanii* (the interclavicles are very similar in PIMUZ T 2475 and PIMUZ T 4355, despite the differences in size, and likely age, of these specimens) in having wide wing-like processes and laterally pointed tips, circular emarginations on the posterior margins of the wing-like processes, anterior rod-like processes that extend from a common base and enclose a narrow V-shaped median notch, as well as a shorter fusiform caudal process, which is expanded in its mid-shaft region and with a rounded posterior tip (Figure 7). It is possible these characters are potentially diagnostic of *M. fuyuanensis* (see above), but they need to be tested against Chinese specimens with a better known interclavicle. Neither IVPP V15001 nor GMPKU-P-3001 shows a well-exposed interclavicle. Whether the bone ornamentation seen in PIMUZ T 4355, absent in PIMUZ T 1559, could potentially be diagnostic for *M. bassanii* cannot be unambiguously elucidated based on the present data. The rounded wing-like processes and the U-shaped median notch seen in the interclavicles of *M. bassanii*, on the other hand, are similar to that of the interclavicles of BP/1/2675 of *Prolacerta broomi* (Ezcurra, 2016: Figure 38 A).

Reconstruction of the Pectoral Girdle

In previous reconstructions of the scapulocoracoid in *Macrocnemus* (Rieppel, 1989; Premru, 1991), both bones were shown with a straight closed contact. This is due to the fact that for most specimens used previously for reconstructing the pectoral girdle the preservation of the bones is not ideal. On the other hand, Ezcurra (2016; p. 219) indicated the presence of a “large fenestra [or embayment] between scapula and coracoid immediately anterior to the glenoid region” in tanystropheids (character 388 in that study). The shape and articulation of the coracoid and scapula based on PIMUZ T 1559 (Figure 11) clearly supports the presence of such a large embayment and indeed, PIMUZ T 2472 does also show a slit-like separation or embayment (contra Rieppel, 1989) between the scapula and coracoid (see Figures 11A–D) due to the distorted shape

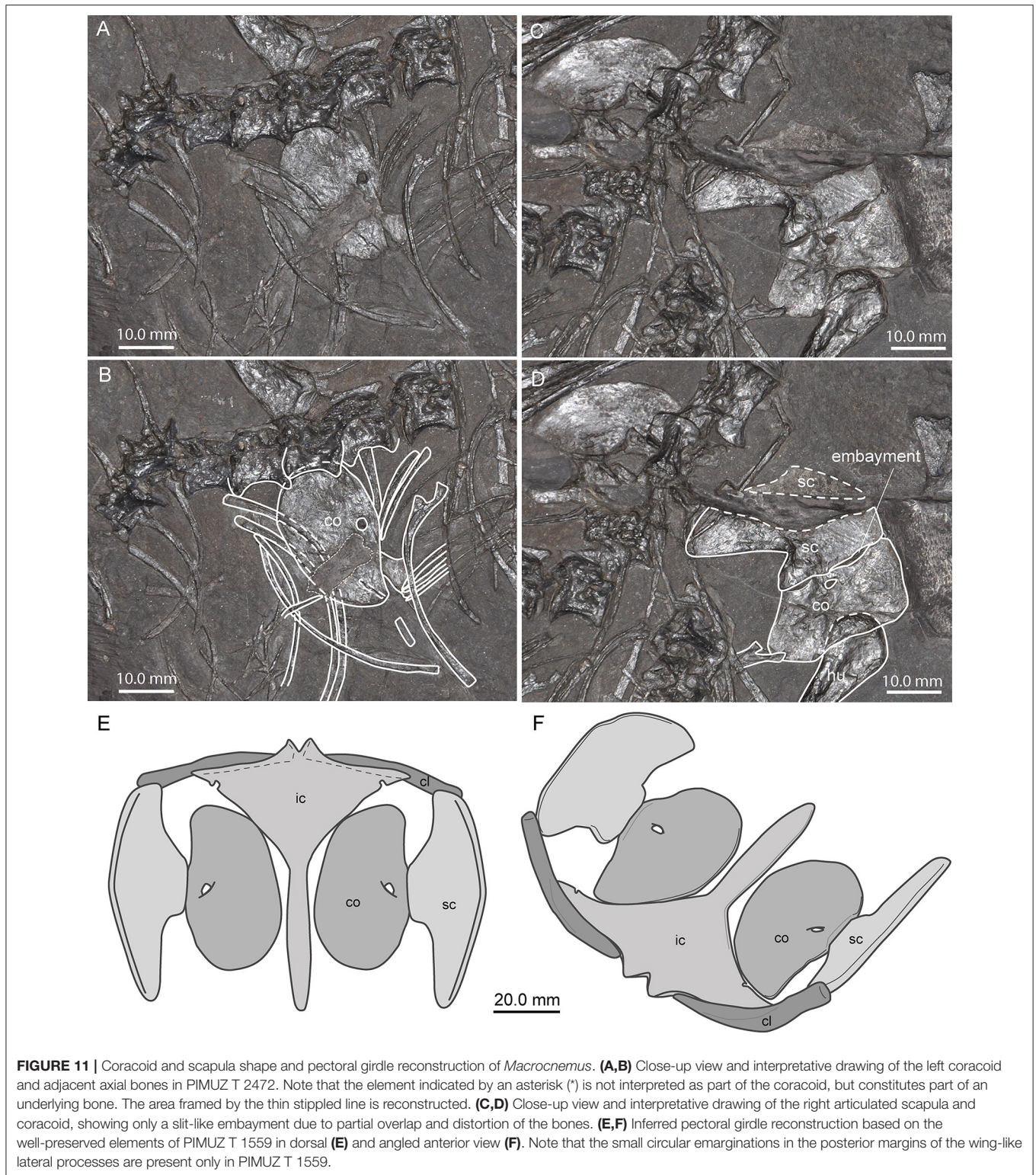
and partial overlap of these bones. The condition in PIMUZ T 4355 (Ezcurra, 2016) and PIMUZ T 2472, together with the new data of PIMUZ T 1559, clearly corroborate the original scapulocoracoid reconstruction given by Peyer (1937).

Furthermore, no specimen of *Macrocnemus* shows the clavicle preserved in articulation with the scapula or interclavicle, so the arrangement inferred by Peyer (1937) was not based on anatomical evidence in the fossils. Peyer (1937) considered it the most probable solution that the thick blunt part of the clavicle articulates with the interclavicle, directly lateral to the anterior processes framing the U-shaped median notch, and the flaring blade-like part of the clavicle articulates with the scapular blade. This configuration was then adopted in later descriptions of *Macrocnemus* (Rieppel, 1989; Premru, 1991) and, for that matter, of *Tanystropheus*, due to the resemblance of the morphology of this element in both taxa (Wild, 1973). However, the well-preserved clavicles and interclavicle of PIMUZ T 1559 allow for a rather different configuration. The long lateral wing-like processes of the interclavicle bear anterior articulation facets for the clavicle, the length of which correspond well with the length of the thin margin on the expanded half of the clavicle. Extant phylogenetic bracketing was considered in order to infer the position of the clavicle, but crocodylians do not possess this element anymore (Mook, 1921; Romer, 1956) and the furcula of birds is highly derived from the basic archosaur plan and variable (Ponton et al., 2007; Nesbitt et al., 2009 and references therein). However, the clavicle of *Macrocnemus* very closely resembles that of the rhynchocephalian *Sphenodon punctatus* (PIMUZ A/III 1007) and the iguanid *Iguana iguana* (PIMUZ A/III 971). In those two taxa the flat convex side of the clavicle also articulates with the interclavicle while the blunt, thickened end reaches the scapula. As such, we take that as reasonable evidence to assume that the clavicle in *Macrocnemus* (and perhaps even in *Tanystropheus*) articulated in a similar way. Together with the scapulocoracoid articulation discussed above, we present here a new pectoral girdle reconstruction for *Macrocnemus* (Figures 11E,F).

Vertebrae

We note a slight disagreement between our and Rieppel's (1989) identification of the cervical vertebrae of PIMUZ T 2472. Whereas, measurements of the individual vertebrae are congruent, the first complete and measurable vertebra seen by Rieppel (1989) is the fourth cervical, which we interpret as the fifth herein. Based on the size of the gap and the average length of the cervical vertebral centra, there is space for another, the third, cervical vertebra next to the missing half of the fourth cervical centrum. This leaves the smaller anterior fragment only interpretable as the axis. The relative size of the latter is comparable to its counterpart in PIMUZ T 1559, and the measurements of the cervical vertebrae of this new specimen further support this view.

In assessing the lengths of the centra of the vertebrae of PIMUZ T 1559, a distinct difference in size can be discerned between centra four to seven (~20 mm), when compared with those of the tenth and more posterior vertebrae (~10 mm).



However, the eighth (~16–17 mm) and ninth vertebra (~13–14 mm) are intermediate in size so that there is not an abrupt change in length. This therefore provides no direct indication where to separate the cervical vertebrae from the dorsal vertebral

column. The best evidence comes from the cervical ribs of PIMUZ T 1559. Only the ribs up to the eighth vertebra are straight, and there is a considerable increase in size from the ribs of the eighth to those of the ninth vertebra. Consequently,

it seems reasonable to define the cervical region to include vertebrae one to eight and the dorsal region to include vertebrae 9–25; with 26 and 27 being the two sacral vertebrae. If this rationale is applied also to PIMUZ T 2472, it implies that this specimen of *M. bassanii* also possesses 17 dorsal vertebrae rather than 16 as reported by Rieppel (1989). The rib on the seventh cervical of PIMUZ T 2472 is very short but broken off posteriorly; an evaluation of the original length is thus impossible. The head of the rib of the eighth vertebra appears to be similar to that of the rib of the ninth in PIMUZ T 1559, but is much shorter as would be expected (see discussion above); the morphological similarity may be due to some distortion of the rib head.

Paleogeography of *Macrocnemus*

The oldest representatives of “protorosaurs,” currently a polyphyletic grouping, are known from the middle Late Permian, namely *Aenigmastropheus parringtoni* from Tanzania and *Protosaurus speneri* from Germany and England (Ezcurra, 2016). On the other hand, Tanystropheidae, according to recent phylogenetic analyses (Nesbitt et al., 2015; Pritchard et al., 2015; Ezcurra, 2016), include at least *M. bassanii* and *Tanystropheus longobardicus* from the upper Anisian—lower Ladinian of Switzerland and Italy, *M. fuyuanensis* from the Ladinian of Yunnan Province, southern China (Li et al., 2007; Jiang et al., 2011), *Langobardisaurus pandolfii* from the Norian of Italy and Austria (Renesto and Dalla Vecchia, 2007; Saller et al., 2013), *Tanytrachelos ahynis* from the Norian of Virginia, USA (Olsen, 1979), new Tanystropheidae remains from the middle Norian of New Mexico, USA (Pritchard et al., 2015) and *Amotosaurus rotfeldensis* from the lower Anisian of Germany (Fraser and Rieppel, 2006). Although not specified in those studies, material of *Augustaburiania vatagini* from the Olenekian of Russia (Sennikov, 2011), *M. obristi* from the lower Ladinian of Switzerland (Fraser and Furrer, 2013), *Tanystropheus* sp. from the Ladinian (Zhuganpo Member of the Falang Formation) and the Carnian to Norian of Italy (Dalla Vecchia, 2000, 2006), as well as *Tanystropheus* cf. *longobardicus* from the upper part of the Zhuganpo Member of Falang Formation of southern China (Rieppel et al., 2010) and *Protanystropheus antiquus* from the Anisian of Poland (Sennikov, 2011) have been described as members of Tanystropheidae. Due to the fragmentary nature of some of the material (i.e., North American Tanystropheidae indet., *Augustaburiania*, and *Protanystropheus*) it is difficult to assess their systematic position and their exact value for palaeobiogeographic inference (see Pritchard et al., 2015 for discussion).

Of all the above mentioned genera, only *Macrocnemus* and *Tanystropheus* are known to occur from both the western and eastern Tethyan province, with the specimens of *M. aff. fuyuanensis* and *T. (cf.) longobardicus* from Europe being slightly older (late Anisian to early Ladinian) than the Chinese specimens (Ladinian). The oldest remains of well-known Tanystropheidae, i.e., *Amotosaurus*, are recovered from the northwestern margin of the western Tethyan province, whereas the sister group to Tanystropheidae (sensu Ezcurra, 2016), *Jesairosaurus lehmani* comes from the Olenekian (Spathian) to

Anisian of Algeria (Jalil, 1997), representing the southwestern margin of the Tethyan province in the Early to Middle Triassic.

In accordance with previous paleogeographic scenarios (e.g., Pritchard et al., 2015) we thus propose that during the late Early Triassic, tanystropheid reptiles first evolved from their Late Permian and Early Triassic ancestors in central Pangaea and first dispersed along the western margin of the Tethys Ocean, before spreading to the eastern margins of the Tethys during the Middle Triassic, whereas dispersal to what is now North America started only later, during the early Late Triassic.

CONCLUSIONS

We record for the first time the occurrence of the Ladinian eastern Tethyan species *M. aff. M. fuyuanensis* from the western Tethys, i.e., the upper Anisian part of the Besano Formation of Europe. Therefore, this taxon is only the second tanystropheid, besides *Tanystropheus* (cf.) *longobardicus* having a Tethys-wide distribution. We furthermore propose that the interclavicle shows characteristic morphologies that allows for separation of *M. bassanii* and *M. aff. M. fuyuanensis* and present a new reconstruction of the pectoral girdle for the genus. On the other hand, the reinterpretation of the skull bone configuration of *M. fuyuanensis* given herein is more consistent with that of *M. bassanii* than previously suggested by Jiang et al. (2011).

Finally, we show that:

- High positive humerus/radius (H/R) ratios (19–21%) are found only in specimens of *M. fuyuanensis* (IVPP V15001, GMPKU-P-3001) and in PIMUZ T 1559 (22%).
- Slightly positive H/R ratios (up to 11%) are present in *M. bassanii* specimens.
- A high positive tibia/femur (T/F) ratio (26%) is only present in *M. obristi* (holotype PIMUZ A/III 1467).
- Slightly positive T/F ratios (up to 12%) are found in *M. bassanii* specimens.
- Equal or slightly negative T/F ratios are found only in specimens of *M. fuyuanensis* from China, although the difference to some specimens of *M. bassanii* with low positive values is negligible (see **Table 6**).

AUTHOR CONTRIBUTIONS

This work was part of the M.Sc. thesis of VJ. TS, and HF designed the study. The analyses were done by VJ, NF, and TS. VJ and TS wrote the manuscript but all authors contributed to the writing and the revision of the text. Figures were prepared by VJ and TS. All authors gave their final approval for publication.

FUNDING

Specimen PIMUZ T 1559 was prepared in the framework of SNSF Synergia grant CRSII3-136293. TS acknowledges funding by the SNSF (grant no. 205321_162775).

ACKNOWLEDGMENTS

Li Chun (IVPP) and Jiang Da-yong (PKU) are thanked for access to the Chinese specimens under their care and for their hospitality and support during visits in Beijing. Christian Klug (PIMUZ) is thanked for access to the material in the PIMUZ collections. T. Brühwiler (PIMUZ) and U. Oberli (St. Gallen) are thanked for the skillful preparation of PIMUZ T 1559. We thank S. Nosotti (MSNM), S. Spiekman, A. Latimer and the “Evolutionary Morphology and

Paleobiology of Vertebrates” working group (all PIMUZ) for fruitful discussions. We also like to thank associate editor Martin Ezcurra and three reviewers for their various helpful comments.

SUPPLEMENTARY MATERIAL

The Supplementary Material for this article can be found online at: <https://www.frontiersin.org/articles/10.3389/feart.2017.00091/full#supplementary-material>

REFERENCES

- Dalla Vecchia, F. M. (2000). *Tanystropheus* (Archosauromorpha, Prolacertiformes) remains from the Triassic of the Northern Friuli (NE Italy). *Riv. Ital. Paleontol. Stratig.* 106, 135–140.
- Dalla Vecchia, F. M. (2006). Resti di *Tanystropheus*, sauroterrigi e “rauisuchi” (Reptilia) nel Triassico medio della Val Aupa (Moggio Udinese, Udine). *Gortania* 27, 25–48.
- Ezcurra, M. D. (2016). The phylogenetic relationships of basal archosauromorphs, with an emphasis on the systematics of proterosuchian archosauriforms. *PeerJ* 4:e1778. doi: 10.7717/peerj.1778
- Fraser, N. C., and Rieppel, O. (2006). A new protosauromorph (Diapsida) from the upper Buntsandstein of the Black Forest, Germany. *J. Vertebr. Paleontol.* 26, 866–871. doi: 10.1671/0272-4634(2006)26[866:ANPDF]2.0.CO;2
- Fraser, N., and Furrer, H. (2013). A new species of *Macrocnemus* from the middle Triassic of the eastern Swiss Alps. *Swiss J. Geosci.* 106, 199–206. doi: 10.1007/s00015-013-0137-5
- Gervais, P. (1859). *Zoologie et Paléontologie Françaises*. Paris: Arthus Bertrand.
- Gottmann-Quesada, A., and Sander, P. M. (2009). A redescription of the early archosauromorph *Protosaurus speneri* MEYER, 1832, and its phylogenetic relationships. *Palaeontographica Abt. A* 287, 123–220. doi: 10.1127/pala/287/2009/123
- Huxley, T. H. (1871). *A Manual of the Anatomy of Vertebrated Animals*. London: J. & A. Churchill.
- Jalil, N.-E. (1997). A new prolacertiform diapsid from the Triassic of North Africa and the interrelationships of the Prolacertiformes. *J. Vertebr. Paleontol.* 17, 506–525. doi: 10.1080/02724634.1997.10010998
- Jiang, D.-Y., Rieppel, O., Fraser, N. C., Motani, R., Hao, W.-C., Tintori, A., et al. (2011). New information on the protosauromorph reptile *Macrocnemus fuyuanensis* Li et al., 2007, from the middle/upper Triassic of Yunnan, China. *J. Vertebr. Paleontol.* 31, 1230–1237. doi: 10.1080/02724634.2011.610853
- Kuhn-Schwyder, E. (1962). Ein weiterer Schädel von *Macrocnemus bassanii* Nopcsa aus der anisischen Stufe der Trias des Monte San Giorgio (Kt. Tessin, Schweiz). *Paläontologische Zeitschrift [Festband Hermann Schmidt zur Vollendung des 70. Lebensjahres am 3. November 1962. Sonderausgabe zur Paläontologischen Zeitschrift, 1962; 265 pp.]*, 110–133.
- Li, C. (2003). First record of protosauromorph reptile (Order Protosauromorpha) from the middle Triassic of China. *Acta Geol. Sin.* 77, 419–423. doi: 10.1111/j.1755-6724.2003.tb00122.x
- Li, C., Rieppel, O., and LaBarbera, M. C. (2004). A Triassic aquatic protosauromorph with an extremely long neck. *Science* 24, 305. doi: 10.1126/science.1100498
- Li, C., Zhao, L., and Wang, L. (2007). A new species of *Macrocnemus* (Reptilia: Protosauromorpha) from the middle Triassic of southwestern China and its palaeogeographical implication. *Sci. China Ser. D* 50, 1601–1605. doi: 10.1007/s11430-007-0118-5
- Mook, C. C. (1921). Notes on the postcranial skeleton in the Crocodilia. *Bull. Am. Mus. Nat. Hist.* 44, 67–100.
- Nesbitt, S. J., Flynn, J. J., Pritchard, A. C., Parrish, J. M., Ranivoharimanana, L., and Wyss, A. R. (2015). Postcranial osteology of *Azendohsaurus madagaskarensis* (?Middle to Upper Triassic, Isalo Group, Madagascar) and its systematic position among stem archosaur reptiles. *Bull. Am. Mus. Nat. Hist.* 398, 1–126. doi: 10.1206/amnb-899-00-1-126.1
- Nesbitt, S. J., Turner, A. H., Spaulding, M., Conrad, J. L., and Norell, M. A. (2009). The theropod furcula. *J. Morphol.* 270, 856–879. doi: 10.1002/jmor.10724
- Nieuwenhuys, R., ten Donkelaar, H. J., and Nicholson, C. (1998). *The Central Nervous System of Vertebrates, Vol. 1*. Berlin: Springer.
- Nopcsa, F. B. (1930). Notizen über *Macrocnemus bassanii* nov. gen. et spec. *Centralblatt für Mineralogie, etc. Abt. B.* 7, 252–255.
- Nopcsa, F. B. (1931). *Macrocnemus* nicht *Macrocnemus*. *Centralblatt für Mineralogie, etc. Abt. B.* 655–656.
- Olsen, P. E. (1979). A new aquatic eosuchian from the Newark Supergroup (Late Triassic-Early Jurassic) of North Carolina and Virginia. *Postilla* 176, 1–14.
- Peyer, B. (1931). *Macrocnemus* nicht *Macrocnemus*. *Centralblatt für Mineralogie, etc. Abt. B.* 4, 190–192.
- Peyer, B. (1937). Die Triasfauna der Tessiner Kalkalpen. XII. *Macrocnemus bassanii* Nopcsa. *Abhand. Schweiz. Paläontol. Ges.* 59, 1–140.
- Ponton, F., Montes, L., Castanet, J., and Cubo, J. (2007). Bone histological correlates of high-frequency flapping flight and body mass in the furculae of birds: a phylogenetic approach. *Biol. J. Linn. Soc.* 91, 729–738. doi: 10.1111/j.1095-8312.2007.00836.x
- Premru, E. (1991). *Beschreibung eines neuen Fundes von Macrocnemus bassanii Nopcsa (Reptilia, Squamata, Prolacertiformes) aus der Grenzbitumenzone (Anis/Ladin) des Monte San Giorgio (Besano, I)*. Diploma thesis, University of Zurich.
- Pritchard, A. C., Turner, A. H., Nesbitt, S. J., Irmis, R. B., and Smith, N. D. (2015). Late Triassic tanystropheids (Reptilia, Archosauromorpha) from northern New Mexico (Petrified forest member, Chinle formation) and the biogeography, functional morphology, and evolution of Tanystropheidae. *J. Vertebr. Paleontol.* 35:e911186. doi: 10.1080/02724634.2014.911186
- Renesto, S., and Avanzini, M. (2002). Skin remains in a juvenile *Macrocnemus bassanii* Nopcsa (Reptilia, Prolacertiformes) from the Middle Triassic of Northern Italy. *Neues Jahrb. Geol. Paläontol. Abh.* 224, 31–48.
- Renesto, S., and Dalla Vecchia, F. M. (2007). A revision of *Langobardisaurus rossii* Bizzarrini and Muscio 1995 from the Late Triassic of Friuli. *Riv. Ital. di Paleontol. Stratigrafia* 113, 191–201.
- Rieppel, O. (1989). The hind limb of *Macrocnemus bassanii* (Nopcsa) (Reptilia, Diapsida): development and functional anatomy. *J. Vertebr. Paleontol.* 9, 373–387. doi: 10.1080/02724634.1989.10011771
- Rieppel, O., and Gronowski, R. W. (1981). The loss of the lower temporal arcade in diapsid reptiles. *Zool. J. Linn. Soc.* 72, 203–217. doi: 10.1111/j.1096-3642.1981.tb01570.x
- Rieppel, O., Jiang, D.-Y., Fraser, N. C., Hao, W.-C., Motani, R., Sun, Y.-L., et al. (2010). *Tanystropheus* cf. *T. longobardicus* from the early late Triassic of Guizhou Province, southwestern China. *J. Vertebr. Paleontol.* 30, 1082–1089. doi: 10.1080/02724634.2010.483548

- Romer, A. S. (1956). *Osteology of the Reptiles*. Chicago: University of Chicago Press.
- Saller, F., Renesto, S., and Dalla Vecchia, F. M. (2013). First record of *Langobardisaurus* (Diapsida, Protorosauria) from the Norian (Late Triassic) of Austria, and a revision of the genus. *N. Jb. Geol. Paläont. Abh.* 268, 83–95. doi: 10.1127/0077-7749/2013/0319
- Sennikov, A. G. (2011). New tanystropheids (Reptilia: Archosauromorpha) from the Triassic of Europe. *Paleontol. J.* 45, 90–104. doi: 10.1134/S0031030111010151
- Wild, R. (1973). E. Kuhn-Schnyder und B. Peyer: die Triasfauna der Tessiner Kalkalpen. XXIII. *Tanystropheus longobardicus* (Bassani) (Neue Ergebnisse). *Schweiz. Paläontol. Abh.* 95, 1–162.

Conflict of Interest Statement: The authors declare that the research was conducted in the absence of any commercial or financial relationships that could be construed as a potential conflict of interest.

The reviewer, FA, and handling Editor declared their shared affiliation.

Copyright © 2017 Jaquier, Fraser, Furrer and Scheyer. This is an open-access article distributed under the terms of the Creative Commons Attribution License (CC BY). The use, distribution or reproduction in other forums is permitted, provided the original author(s) or licensor are credited and that the original publication in this journal is cited, in accordance with accepted academic practice. No use, distribution or reproduction is permitted which does not comply with these terms.